University of Crete

Department of Biology

FORTH

Institute of Molecular Biology & Biotechnology (IMBB)

Master of Science (MSc):

"Molecular Biology-Biomedicine"

MASTER THESIS

Title: Role of Myelination in Hippocampal Inhibitory Neurons.

Advisor: Dr. Domna Karagogeos

Supervisor: Dr. Domna Karagogeos & Dr. Theodora Velona

Author: Sofia Petsangouraki

Heraklion, 2021

Περίληψη

Οι ενδονευρώνες, είναι ανασταλτικοί νευρώνες που εκλύουν τον νευροδιαβιβαστή γ-αμινοβουτυρικό οξύ (GABA) και αποτελούν το 10-15% του συνολικού αριθμού των κυττάρων του νευρικού συστήματος. Παρόλο το μικρό τους αριθμό είναι αναγκαίοι για την ισορροπία ανάμεσα σε διέγερση και αναστολή στο νευρικό σύστημα και για την πρόληψη ενάντια σε δυνητική υπερδιέγερση και τοξικότητα. Έτσι καθίστανται ευάλωτοι σε αλλοιώσεις που οδηγούν σε νευροεκφυλιστικές ασθένειες.

Προσφάτως, ανακαλύφθηκε πως ένα μεγάλο μέρος της μυελίνης του νεοφλοιού και του ιππόκαμπου μυών και ανθρώπων αποδίδεται στους ενδονευρώνες όπως τους παρβαλβουμίνικούς (Parvalvumin, PV), υπονοώντας την εμπλοκή τους σε απομυελινωτικές ασθένειες. Η μυελίνη είναι λιποειδείς μεμβρανώδεις προεκτάσεις της πλασματικής μεμβράνης των ολιγοδρνδροκυττάρων στο κεντρικό νευρικό σύστημα (ΚΝΣ) και των κυττάρων Schwan στην περιφέρεια, που περικλείουν τους νευράξονες. Το περίβλημα αυτό είναι υπεύθυνο για την μόνωση, τη γρήγορη μεταγωγή δυναμικών ενεργείας και τη μεταβολική υποστήριξη των νευρικών αξόνων. Η διαδικασία εναπόθεσης μυελίνης στους νευράξονες είναι γνωστή και ως μυελίνωση.

Η μυέλινή των διάμεσων νευρώνων είναι διακοπτόμενη διαφέροντας από εκείνη των διεγερτικών νευρώνων ενώ, ο μηχανισμός της μυελίνωσης καθώς και ο τρόπος κατάληψης των Κόμβων του Ranvier και των παρακομβικών περιοχών από τα πρωτεϊνικά τους συστατικά, παραμένει άγνωστος. Περαιτέρω μελέτες στους διάμεσους νευρώνες του ιππόκαμπου έδειξαν την παρουσία πρωτεϊνικών συστατικών των εγγύς παρακομβικών περιοχών, και πιο συγκεκριμένα την επιλεκτική έκφραση της πρωτεΐνης TAG-1/CNTN2 της οικογένειας των ανοσοσφαιρινών σε αυτές τις περιοχές.

Μέσα από την παρούσα εργασία επιδιώκουμε 1) την κατανόηση του ρόλου της μυελίνης στους ενδονευρώνες κατά την ωρίμανση τους και ταυτόχρονα θέτουμε τις βάσεις για την 2) κατανόηση της λειτουργίας των εμμύελων ενδονευρώνων μέσα από μοντέλα απομυελίνωσης ή δυσλειτουργικής μυελίνωσης.

Λέξεις Κλειδιά: Μυελίνωση, Ενδονευρώνες, Απομυελίνωση, TAG-1, ιππόκαμπος, Parvalbumin (PV)

Abstract

Interneurons are inhibitory neurons that release the neurotransmitter γ-aminobutyric acid (GABA) and make up 10-15% of the total number of cells in the nervous system. Despite their small population, they are necessary for the balance between excitation and inhibition in the nervous system and for the prevention of potential overexcitation and toxicity. Thus they become vulnerable to others leading to neurodegenerative diseases.

Recently, it has been discovered that a large part of the myelin of the neocortex and hippocampus of mice and humans is attributed to interneurons such as parvalvumin (PV), implying their involvement in demyelinating diseases. Myelin is lipid-rich membranous extension of the plasma membrane of oligodrondrocytes in the central nervous system (CNS) and Schwann cells in the periphery, enclosing the axons. Myelin sheaths are responsible for the insulation, rapid conversion of energy potentials and the metabolic support of the axons. The process of myelin deposition in the axons is also known as myelination.

The myelin of interneurons differs from that of excitatory neurons, while the mechanism of myelination as well as the way in which the Ranvier Nodes and the perinodal areas are occupied by their protein components remains unknown. Further studies on hippocampal inhibitory neurons have shown the presence of protein components in the proximal regions, and more specifically the selective expression of the TAG-1 / CNTN2 protein of the immunoglobulin family in these regions.

Through the present work we seek 1) the understanding of the role of myelin in the interneurons during their maturation and at the same time we lay the foundation for 2) the understanding of the function of the medullary interneurons through models of demyelination or dysfunctional myelination.

Key words: Myelination, Interneurons, demyelination TAG-1, hippocampus, Parvalbumin(PV)

Index

1. Introduction 6
   1.1 Hippocampus: 6
      1.1.1 Brain Areas & Role 6
      1.1.2 Circuity 8
      1.1.3 Cornu Ammonis 1 (CA1) 9
      1.1.4 Parvalbumin Interneurons 11
   1.2 Relationship between Interneurons and Oligodendrocytes 15
   1.3 Myelination: types & role 16
   1.4 Myelin spatial and molecular organization 20
   1.5 Contactin 2 (CNTN2) or TAG-1 21
      1.4.1 TAG-1 mouse line 23
2. Materials and Methods 24
   2.1 Animals 24
   2.2 DNA extraction & Genotyping 24
   2.3 Tissue fixation, isolation, cryoprotection 26
   2.4 Tissue Embedding, Freezing, Cryosectioning 26
   2.5 Immunohistochemistry on cryosections 26
   2.6 Hippocampus dissection 28
   2.7 Western Blotting 29
      2.7.1 Tissue preparation 29
      2.7.2 Running 30
      2.7.3 Transfer 30
      2.7.4 Immunoblot & Imaging/ Detection 31
   2.8 Lysophosphatidylcholine (LPC) injection 32
   2.8 Electron Microscopy (EM) sample preparation 34
      2.8.1 Animal Perfusion 34
      2.8.2 Washes 34
      2.8.3 Vibratome sections preparation & Tissue cryoprotection 34
      2.8.4 Freeze thawing and incubation with the 1st Antibody 35
      2.8.5 Incubation with Secondary Antibody 35
      2.8.6 Silver Enhancement, Processing with Osmium/Uranium, Tissue Embedding 36
      2.8.7 Tissue Re-embedding 38
3. Objective 39
4. Results 39

4.1 Role of TAG-1 in PV interneurons 39
4.2 Number of Parvalbumin interneurons cells in the hippocampus 41
4.3 Myelin morphology of PV interneurons in Tag1 deficient animals 42
4.4 Vulnerability of PV axons to demyelination 43
5. Discussion 44

1. Introduction

1.1 Hippocampus:

1.1.1 Brain Areas & Role

The hippocampus, a bulb-like structure in rodents, is located just beneath the neocortex and was first studied as the pre-eminent model of the cellular basis of memory, an idea that was further elucidated after the discovery of place cells, head direction cells, and grid cells. The hippocampus proper is composed of two major areas, the dentate gyrus (DG) and the Cornu Ammonis (CA). When referring to hippocampal formation, the hippocampus

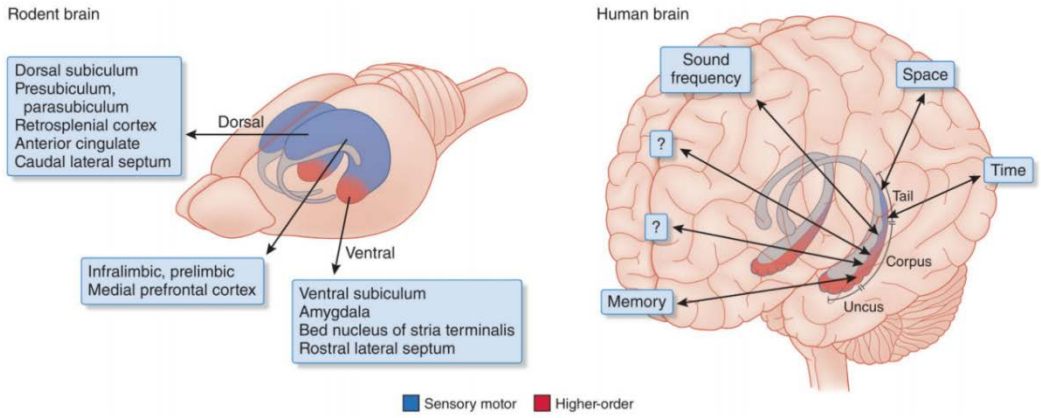

Figure 1: Homologous regions of the hippocampus in the human and rat brains. (J.Lisman et al, 2017)

subiculum (Latin for "support"), pre-subiculum, para-subiculum and entorhinal cortex are included (Fig.1).

The hippocampus is known to be critical in memory processing, learning, and emotions. It is characterized by a specific lamination, the intraventricular part of the hippocampus being covered by a thin layer of white matter that consists of the alveus, containing afferent and efferent hippocampal fibers and forming the floor of the temporal horn of the lateral ventricle. The CA is divided into four cortical fields: CA1, CA2, CA3, and CA4 with discrete lamination in strata with distinct neuron morphology, connectivity and electrophysiological profiles (Khalaf-Nazzal R. & Francis F. 2013).

Hippocampal subdomains are established during development where specific molecular markers are expressed that correspond to different cell populations. These markers are tightly related to functionality and thus are used as molecular boundaries among the various subpopulations (Thompson C.L. et al., 2008). In developmental stages of hippocampus, the transitions of one pyramidal cell type to another is sufficient to mark both morphological

and molecular changes from CA1 to CA3. CA2 expresses other specific molecular markers that define the area, its function and thus its identity (Wyszynski M. et al., 1997). For instance, studies have shown two intense and specialized markers to be expressed in the pyramidal neurons of CA3 and CA1. The KA1, a glutamate receptor subunit, which is expressed in the former and the SCIP, a POU-domain gene expressed in the latter (Tole S, Christian C, Grove EA, 1997). These two serve as markers in both development and adult stages. In addition, the Wnt3a signaling pathway is critical in early development of the hippocampal formation because it extends in the developing fields, while the cortical hem - source of Wnt (Wingless) and BMP (bone morphogenetic protein) in the dorsomedial telencephalon- expresses signals required for hippocampal field specification and growth (Tole S. and Grove E. A., 2001).

In the hippocampus, multiple cells from different lineages and regions coexist, whose neurogenesis starts early, at E10 in mice. More precisely, Cajal-Retzius (CR) cells comprise a cellular population expressed transiently in both cerebral cortex and hippocampus. Among others it is the first neuronal subtype generated in the developing telencephalon at three different sites that function as patterning centers. Their principal function relies in the guidance of migrating neurons or acting as progenitor cells and on the regulation of glial morphology. Another neuronal population is the hippocampal projection neurons, which are characterized by wide diversity in terms of location, distribution, molecular markers and properties. As for their morphogenesis, they differentiate from bipolar to more complex morphologies that characterize adult cells providing functional differentiation as well. The third class of cells is the dentate gyrus cells. These cells are generated in the neuroepithelium, close to the fimbria. The development of DG starts at E10 developmental stage, while their accumulation in the DG area become obvious at E18. The last cell population is the hippocampal interneurons which are divided into several categories depending on their axonal projection pattern, neurochemical content and physiological properties. Due to the variability of hippocampal interneurons and their specific circuit patterns, scientists believe that their identities are shaped during development and these identities are space and time dependent. As for their function, they recognize pyramidal membrane signatures to establish inhibitory connections (Khalaf-Nazzal R. & Francis F. 2013).

1.1.2 Circuitry

The entorhinal cortex is the biggest source of inputs provided to the hippocampus, with its strongest projections via the perforant path to the dentate gyrus (DG) region (Synapse 1). The DG projects to the CA3 region via the mossy fiber pathway (Synapse 2). CA3 projects to the CA1 region via the Schaffer Collateral pathway (Synapse 3). In the end, the loop is completed when CA1 projects back to the entorhinal cortex (Fig.2) (Andersen P. et al 2007, J J Knierim, 2015). An important fact of this tri-synaptic circuity (layer II – DG – CA3 – CA1), is that CA3 axons, in addition to their projections to CA1, send collaterals that make synapses onto other CA3 neurons, a pathway -otherwise known as recurrent collateral pathway- that favors the hypothesis of the CA3 auto-associative memory system, displaying attractor dynamics that are critical for supporting a distributed memory (Knierim J. J., 2015). Apart from the tri-synaptic circuity, a bi-synaptic circuit came to the front. It seems that it involves the CA2 hippocampal area which remains unexplored, but may function as a link between CA3 and CA1 (layer III – CA2 – CA1 pathway) (Sekino Y. et al., 1997).

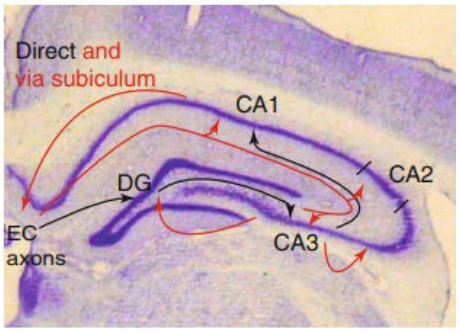

***Figure 2**: Coronal Slice of the hippocampus. The black lines trace the classic 'tri-synaptic' circuitry. The red lines depict other important pathways in the hippocampus, such as the direct projections from entorhinal cortex (EC) to all three CA fields, the feedback to the EC via the subiculum, the recurrent collateral circuitry of CA3, and the feedback projection from CA3 to DG. (Knierim J J, 2015)*

1.1.2.1 Entorhinal Cortex inputs and outputs

As mentioned above, the hippocampus receives many signals from the entorhinal cortex. It is composed of two distinct brain regions in rats. The medial entorhinal cortex (MEC), especially its caudally located regions, is associated with spatial processing areas of the brain, such as the retrosplenial cortex and the dorsal presubiculum (also called the postsubiculum). The lateral entorhinal cortex (LEC) is associated with high-order, item-recognition areas, such as the perirhinal cortex. These two regions receive input from the prefrontal cortex and olfactory cortex, and they also send projections to each other. The MEC and LEC projections to DG and CA3 overlap, appearing to target the same cells. Thus, DG and CA3 can combine the information conveyed by both inputs. On the other hand, the projections to CA1 are segregated along the transverse axis, as the part of CA1 close to the

subiculum receives input from LEC and the part of CA1 close to CA2 receives input from MEC (Fig.3). The superficial layers of MEC and LEC project to the hippocampus (in general, layer II projects to DG and CA3, whereas layer III projects to CA1 and subiculum). The deep layers receive feedback from the hippocampus. Connections from deep to superficial layers, as well as the presence of basal dendrites of layer II/III neurons in deep layers, form a critical anatomical feedback loop that allows the hippocampal output to directly affect the neural processing of the hippocampal inputs (Knierim J.J. 2015)

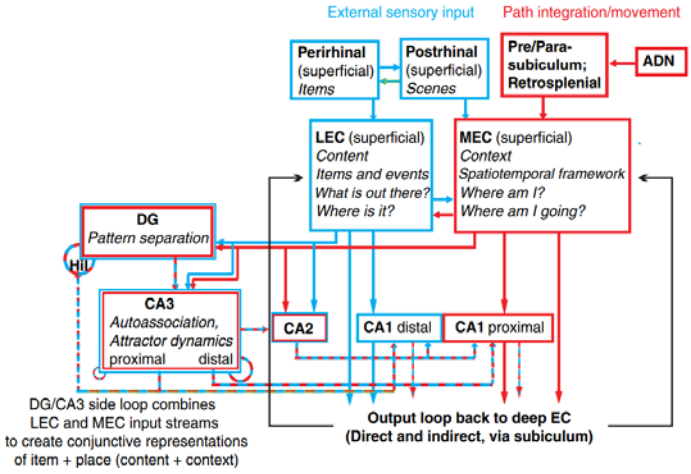

***Figure 3**: Schematic representation of information circulation and function of distinct hippocampal areas that are implicated in memory. In light blue is depicted the Lateral Entorhinal Cortex (LEC) where signals from perirhinal cortex arrive. Information that is related to individual items or events like spatial location is related to this area. As for the Medial Entorhinal Cortex (MEC), pathway that is represented in red, takes signals from postrhinal cortex and is related to self-movement, head direction and path integration from different subiculum subareas. Additionally, data are consigned to DG and CA3 from both pathways, so memory deriving from an experience and its spaciotemporal content is stored like accumulative representations. Also, networks from CA3 are related to memory systems, while the output from both DG and CA3 is leaded to CA1 either directly or indirectly and from there right back to EC. From the EC, information is travelling along neocortical areas where memory processing might be influenced. (Knierim J J, 2015)*

1.1.3 Cornu Ammonis 1 (CA1)

The CA1 extends from the cortex of the parahippocampal gyrus at the subiculum, which is separated from the hippocampus by the hippocampal sulcus. There is a surplus type of classification concerning the subareas of cornu ammonis according to their susceptibility to hypoxia. More precisely, CA1 appears to have a more vulnerable phenotype to hypoxia while on the other hand, CA3 has a more resistant one (Tatu L.& Vuillier F. 2014). The CA1 is part of tri-synaptic pathway that originates from entorhinal cortex. As is already said, it receives inputs from 1) the Schaffer collaterals from CA3, that they project in str. radiatum where

they make synapses and 2) from L3 of the medial entorhinal cortex (mEC), conveying to the str. L-M, and CA2 synapsing in the str. oriens and 3) from CA1 recurrent axons that terminate in the str. oriens mostly on Interneurons (Takacs V.T. et al., 2012).

It is composed principally of pyramidal excitatory glutamatergic neurons together with plenty of GABAergic inhibitory interneurons which are known for their heterogeneity. It has a characteristic lamination pattern resulting from the tight packaging of pyramidal cells (Amaral D.G. & Witter M.P., 1989). Regarding its laminar organization, it is composed of five lamina, alveus, stratum oriens, pyramidale, radiatum and lacunosum-moleculare. The somata of pyramidal cells are located at the stratum pyramidale. From these somata a large caliber apical dendrite extending to the stratum radiatum is generated and many basal dendrites extending to the stratum oriens while their axon can either originate from the soma or from a proximal dendrite (Thome C. et al., 2018). Axons, eventually, pass through the oriens and project in the alveus.

Inhibitory neurons are divided into two main categories depending on their developmental origin. Hippocampal interneurons mainly arise from either medial ganglionic eminence (MGE), from caudal ganglionic eminence (CGE) or from both of these developmental progenitor pools. The majority of MGE-related interneuron progenitors are characterized by the expression of the homeodomain transcription factor Nkx2.1, that is crucial for their differentiation. In the absence of Nkx2.1 the most affected subtypes are the Parvalbumin (PV) and Somatostatin (SST) not only of the hippocampus but of the neocortex as well. MGE-related interneurons are vulnerable in the absence of Lhx6 as well, transcriptor factor, found downstream the Nkx2.1, due to the impaired migration of PV and SST at their final destination (Narboux-Neme N. et. al., 2012). As for their migration, many mechanisms act together to guide interneurons following a tangential type of migration, and eventually, reach their final destination via radial migration obeying to chemoattractants (for instance the Cxcl12 chemokine that attracts interneurons within the IZ/SVZ and MZ, until they mature to begin then radial migration) in the developing hippocampus.

Interneurons exhibit high variability morphologically as well as functionally along the CA1. The CA1 is mainly composed of 29 known interneuron subtypes, with definite morphology and properties, neurochemistry and connectivity (Booker S.A. & Vida I. 2018). Inhibitory neurons arising from the MGE account for 60% of interneurons located at the hippocampus and being parsed in several classes according to their morphology: namely, axo-axonic / chandelier cells which account for the 4% of CA1 hippocampal interneurons , parvalbumin-expressing basket cells make up 14% of CA1 located interneurons , bistratified

cells estimated to make up approximately 6% of these neurons, neurogliaform 9% and ivy cells are related to neurogliaform that constitute the larger group, 23% of the hippocampal GABAergic neurons and finally, oriens lacunosum-moleculare interneurons which are comprise 4.5% of CA1-related inhibitory cells (Pelkey K. A. et al., 2017).

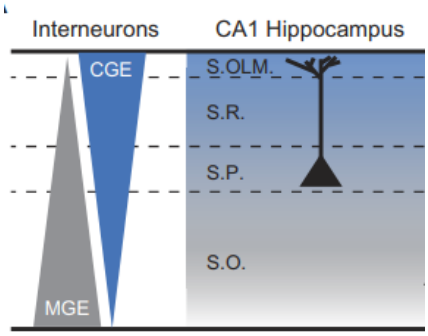

Figure 4: MGE- and CGE-derived interneurons that reach different lamina deep or superficial, respectively. In the hippocampus, lamination depth is relative to the direction of the apical dendrite. (Pelkey K. A. et al., 2017)

1.1.4 Parvalbumin Interneurons

All different subpopulations of GABAergic interneurons act synergistically to regulate the activity of other neurons. Apart from their origin, they can also be divided into subpopulations depending on expression of neuromodulators, like neuropeptides (somatostatin, cholecystokinin etc.) and binding proteins (parvalbumin, calretinin and calbindin), that determine how interneurons operate in a neural network. From the cohort of CA1 interneurons, only 11% of them are GABAergic, while 24% of those inhibitory neurons are Parvalbumin Interneurons (PV-INs) (Bezaire M. J. & Soltesz I. 2013).

Parvalbumin interneurons are a type of inhibitory neurons that express the 12kDa calcium (Ca^{2+}), parvalbumin binding protein. Under physiological conditions, parvalbumin (PV) augments the level of calcium and thus decreases the levels of presynaptic Ca^{2+} and modulates temporal synaptic plasticity and simultaneously prevents fasciculation (fig.5) (Caillard O. et. al., 2000). Due to this property, PV decreases the Ca^{2+}-activated potassium conductance, which is important for post-spike hyperpolarization. This explains partially the reason why PV-Ins repolarize and fire faster than other cells. Therefore, their characteristic phenotype is fast-spiking action potentials that might be costly energy wise (Hu H. et. al.,2014). Such interneurons display a number of electrophysiological properties such as low input resistance (R_{in}), short membrane time constants(τ_m), narrow action potentials and high maximum firing sequency that respond to depolarizing current pulses (Bjorefeldt A. et. al.,2016). PV interneurons have high energy needs in order to support their extreme metabolic activity and, by extension, to protect themselves against glutamatergic stress. Thus, to fill high energy requirements and to preserve gamma oscillations, a high number of

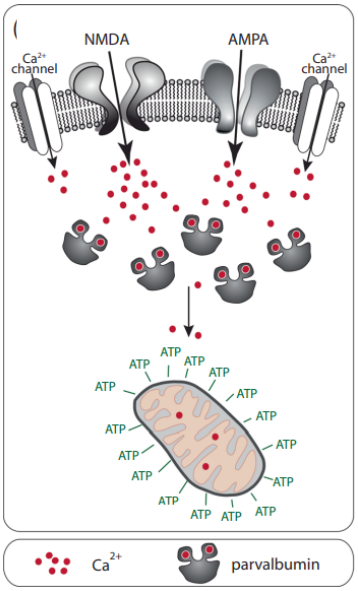

***Figure 5**: Normal quantity of Parvalbumin within interneurons, which buffers the Ca2+ entering through channels / receptors. Due to this Ca2+ stays at normal levels within the mitochondria where ATP is later on produced (Ruden J.B. et. al., 2021).*

mitochondria is needed. Finally, a quantity of cytochrome c and cytochrome c oxidase are important for the endorsement of high energy requirements of such interneurons as well (Ruden J.B. et. al., 2021).

PV inhibitory neurons originate from ganglionic eminences like the majority of GABAergic interneurons from progenitor cells of the developing brain. It seems that they acquire their fate early, from their origin, when progenitors differentiate and leave the cell cycle (Wonders C.P. & Anderson S.A. 2006). During their migration, they receive a slew of attractant and repellant guidance cues deriving from distinct brain areas, that help them to eventually reach their final destination. Simultaneously, the reaction to neuronal cues demands the appropriate timing with the intracellular processes for the expression of the suitable receptors. These receptors are responsible for the downstream regulation of gene expression for microtubule remodeling and actin cytoskeletal activation (Peyer S.E. et. al., 2015). By the time they have reached their final destination, a transcriptome switch starts, which leads to axon pathfinding, synaptic connections with neighboring neurons (Hu J.S. et. al.,2015). Their transcriptomic profile is determined early during development and thus upon perturbed migration, they attenuate their self-renewal or de-differentiation capacities. Since the hippocampus is the most distant area that interneurons have to settle, it is more probable to be affected by impaired migration (Ruden J.B. et. al., 2021).

Regarding their morphological characteristics, PV expressing interneurons of the CA1 hippocampal area are composed of enriched dendritic trees, thicker dendrites and higher density inputs, more excitatory and inhibitory synapses as well as a higher ratio of inhibitory to excitatory inputs than other interneurons such as calbindin or calretinin (Gulyas A.I. et.al.,1999). Parvalbumin interneurons connect many types of neurons by synchronizing principal neuron activity and by being implicated in energy-consuming selection of information and noise dissociation (Ruden J.B. et. al., 2021). They are further categorized in three main cell types: Axo-axonic (AAC) / Chandellier cells, Parvalbumin-Expressing Basket Cells (PVBCs) and Bistratified cells (BiCs).

In the hippocampus, all Axo-axonic / Chandellier cells likewise the Parvalbumin Basket

and Bistratified cells, express parvalbumin. Their cell bodies are principally located at the str. pyramidale and oriens from where dendrites form without spines, with a radial orientation extending from the alveus to the str. lacunosum moleculare while their branches are principally found in the str. radiatum. From the str. l-m they receive excitatory cues from all excitatory afferent nerve endings innervating the whole CA1 area. Their axons can either arise from the soma or a primate dendrite innervating the axon initial segment of up to 1.200 pyramidal cells. Their branches along s.p.-s.o. can run horizontally and project processes from where outgrowths up to 15 boutons that end up to a pyramidal cell (Kenneth P.A. et. al., 2017).

Regarding the Parvalbumin-expressing Basket Cells (PVBCs), they have pyramidal shaped / fusiform somas that are mainly located at the s.p. and s.o. and some of them are found at the s.radiatum. Each cell is connected to up to 2.500 pyramidal cells that form in average 6 synapses onto each pyramidal cell. Their axons are highly concentrated much like the str. radiatum and str. oriens. This type of interneurons account for the approximately 60% of the total number of INs of the CA1 area. The different expression levels of PV, in PVBCs indicate the activity levels of these interneurons within the circuits (Kenneth P.A. et. al., 2017).

The last PV-related interneuron subtype, is the one of Bistratified cells, whose name derives from their axonal arborization innervating both basal and apical dendrites of pyramidal cells. Most of their cell bodies are located at the str. pyramidale and their multipolar dendrites at str. oriens and radiatum. The axons of BiCs contrary to those of AACs and PVBCs avoid the str. l.m and typically their somata are found within the str. oriens while they extend their dendrites horizontally and are mostly found at the str. oriens. They usually are primarily connected to pyramidal cell dendrites usually onto spines. Contrary to AACs and PVBCs, BiCs express and other neuromodulators such as the neuropeptide Y (NPY) and SST as well (Kenneth P.A. et. al., 2017).

Importantly, many interneurons have been found to be implicated in different developmental disorders. PV interneurons have been implicated in the pathophysiology of Schizophrenia (SZ), Alzheimer's disease (AD), autism spectrum disorder (ASD) and bipolar disorder (BPD). In detail, in SZ, they detected a lower quantity of mRNA of PV interneurons not only in the hippocampus but also in entorhinal cortex and subiculum (Konradi C et.al., 2011). As for AD, the mRNA levels of PV-Ins were reduced and at the same time changes in the gamma-oscillations of fast spiking INs were noticed (Iaccarino H.F. et.al., 2016). In contrast the ASD and BPD are two syndromes that share similarities with SZ not only on a

clinical basis but also in PV-INs abnormalities (Crescenco F.et. al., 2019). Apart from the above brain-disorders, epilepsy and prion disease are also related to PV-INs (Sloviter S.R. et.al.,1991).

It was recently found that many GABAergic inhibitory neurons are myelinated in the cortex. Micheva and colleagues, (2016), using light and electron microscopy have shown that a large amount of myelin, that was spotted within the neocortex and especially in layers 2/3 and 4, belongs to interneurons and more precisely to parvalbumin + -basket cells. Interestingly, this type of myelination is discontinuous, with a patchy-like appearance. Their protein arrangement differs from non-GABA neurons, with the MBP(Myelin Basic Protein)protein to be expressed 20% higher in GABA inhibitory neurons. In the case of PLP, its levels revealed no difference between the two neuronal populations (Ruden J.B. et. al., 2021). Additionally, the myelination of GABAergic interneurons is a process that is region-dependent. In the CA1, 80% of myelin located at the str. pyramidale and str. radiatum originates from PV interneurons (Stedehouder J. et.al.,2017). Later on, Bonetto G. et. al. 2019 showed that in hippocampal PV interneurons at the str. pyramidale of the CA1 located express the adhesion moleculeTAG-1 (fig.6) that does not appear in other strata like lacunosum-moleculare. Also, in hippocampal cultures they have shown that PV and SST interneurons express cell adhesion molecules such us the Casp2 and Kv1 channels (fig.7).

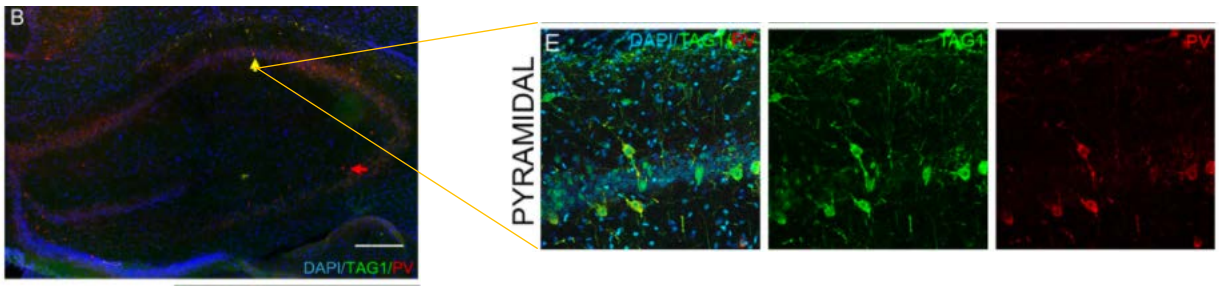

***Figure 6**: B. Coronal cryosections from P21 rat labelled for TAG-1 in green and for PV in red. Scale bar: 50μm E. Magnification of the coronal section in the str. pyramidale, showing the PV (red) co-localization with TAG-1 (green),showing several PV interneurons are TAG-1 positive. Scale bar: 80μm*

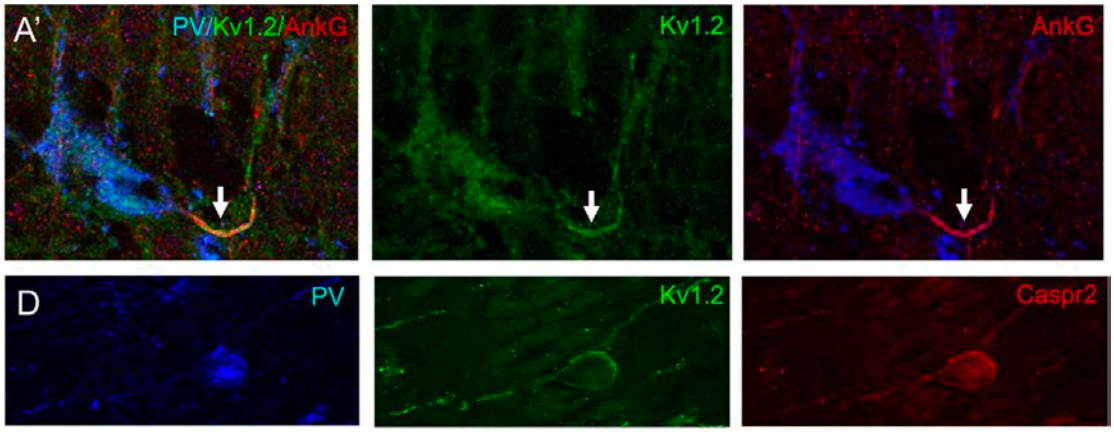

***Figure 7**: A'. staining for AnkG and KV1.2 channels at the AIS of CA1 interneurons located at the str. pyramidale of rat hippocampus. D. Co-expression of Caspr2 and Kv1.2 channels in PV expressing interneurons of the CA1 hippocampal area. Scale bar:15μm*

1.2 Relationship of Interneurons with Oligodendrocytes

Oligodendrocytes are the cells responsible for the myelination of axons. They arise from Oligodendrocyte Precursors Cells (OPCs) which sense their environment for signals from neighboring neurons through different communication mechanisms and eventually, alter their function or properties. OPCs receive both synaptic and non-synaptic inputs from neurons which are able to modulate their function and myelination (Habermacher C. et. al., 2019).

A couple of years ago, scientists have shown that OPCs and interneurons share the same origin. Precisely, OPCs either derive from MGE, LGE, CGE or embryonic preoptic area (POA) but their first wave arises from the MGE at embryonic day (E12.5) under the control of Nkx2.1 transcription factor. Interneurons, as already mentioned, originate from the ganglionic eminences as well (Kessaris N, et. al., 2006). Approximately, 70% of interneurons are subjected in genomic regulation that depends in Nkx2.1 transcription factor (Wamsley B. and Fishell G. 2017). From those 60% originate from the MGE, which mainly gives rise to PV- and SST- interneurons. MGE-derived interneurons and OPCs seems to have more possibilities for interactions because they show "preference" in establishing connections and communication with each other than with other interneurons/oligodendroglia from different eminences. In addition to shared origins, interneurons and OPCs share common migratory routes and sustain regulation of their numbers.

It seems that PV interneurons have a tendency to connect with OPCs that is not noticed in other interneurons. Although, PV interneurons were found to be myelinated in the cortex (Micheva C. et.al., 2016), their preference in synapsing with OPCs is not important

for the intrinsic myelination because OPCs receive synapses from non-myelinated PV interneurons. Their Interaction is not necessary for oligodendrogenesis (Balia M. et. al., 2017) but in myelination, maturation, and development. Finally, as mentioned earlier, PV-interneurons malfunctions in patients with neurodevelopmental disorders, like schizophrenia. Apart from alterations in PV interneurons, impairment of OLs and myelin was also noticed in these disorders (Field D.R. 2008).

1.3 Myelination: types & role

Oligodendrocytes (OLs), a type of the large family of glia cells, located in the Central

Nervous System (CNS) and Schwann cells in the Peripheral Nervous system (PNS), support

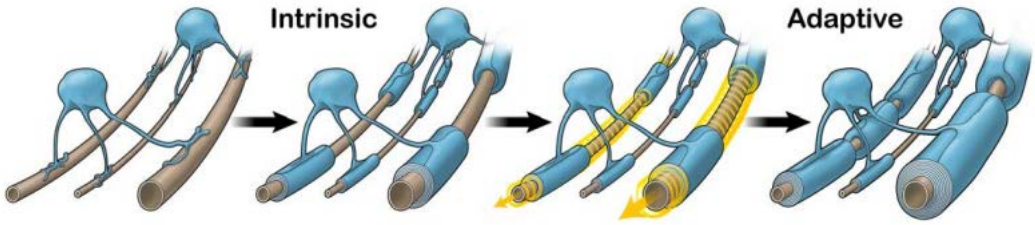

***Figure 8**: Proposed model from Bechler and colleagues for intrinsic and adaptive myelination in the CNS. The demonstrate sequential intrinsic and adaptive pathways that produce "smart" wiring. This model is correlated to activity and also enables learning, through synaptic plasticity. (Bechler M.E. et. al., 2018)*

neurons as well as signal transmission by enwrapping axons with myelin- a process known as myelination. Myelin is a multi-lamellar, lipid rich membrane elaborated by the plasma membrane of OLs in the CNS. It promotes rapid, saltatory conduction of action potentials over long distances (Huxley A.F. & Stampfli R., 1949), by concentrating voltage-dependent sodium channels at the nodes of Ranvier. Many more purposes of myelin have been revealed over the years, for instance its implication in fine tuning neuronal network function (Aiman S. Saab et al, 2016) by synchronizing the firing pattern, while it simultaneously provides metabolic support and protection to the axon (L. Pellerin et al, 1996).

CNS myelination is divided into two categories, the intrinsic and the adaptive phase. The former, is genetically determined, occurs around birth and early childhood and is topologically, and chronologically fixed. During the intrinsic phase, cues for intrinsic myelination from oligodendrocyte precursors cells, drive the differentiation of oligodendrocytes and axonal myelination. OLs detect the axons that are about to be myelinated, by recognizing morphological properties such as axon diameter. They form myelin sheaths equivalent to OL calibers, a phenomenon that is strictly correlated to their transcriptional programming prior to their differentiation (Bechler M. E. et al., 2015).

The latter, comprises the second phase of CNS myelination, and is responsible for the adaptation of already existent-intrinsic myelin sheaths. During adaptation, myelin is plastic, namely modified, during life through external signaling concerning principally their activity, deriving from active neurons. This interaction leads to modulation of myelin sheath in terms of number and size. Thus, myelination levels are diverse among individuals not only due to the different identity among myelinated axons but also due to the adaptive signal each axon receives in adaptive myelination. Eventually a "smart wiring" model is created, in which already myelinated axons, are subjected to changes of their myelin sheath thickness (fig.8) (Bechler M.E. et. al., 2018).

1.4 Myelin: spatial and molecular organization

Myelinated axons are characterized by organizational specializations, because they have a uniform axonal compartmentalization. Precisely, all myelinated axons are composed of the nodes of Ranvier, the paranodes, the juxtaparanodes and the internodes. Regarding the nodes of Ranvier, which are approximately 1μm long, is the axonal area where aggregates of voltage-gated sodium channels (Na_v) are located. This area is myelin-free and thus permits the saltatory conduction of axon potentials along the myelinated axon. In order for an axon potential to occur two phenomena are crucial: firstly the formation of myelin sheaths by oligodendrocytes (in the CNS) and secondly the clustering of Na_v . Components of the Ranvier nodes such as Na_v, two isoforms of Neurofascin, Nfasc186 and Nfasc140, contactin 1 (CNTN1) and cytoskeletal proteins (βIV spectrin and AnkyrinG), several subtypes of voltage-gated potassium channels (Kv.7) are localized at this area during myelination (Ghosh A. et. al., 2018).

As for the paranodes, they are located right next and bilaterally to the nodes of Ranvier. It is the principal area of interaction between the oligodendrocytes and the axolemma. In between is located the biggest intercellular complex of the vertebrates, which is composed of glial Nfasc155, axonal Contactin-associated protein 1 (Caspr, a neurexin family member), and axonal CNTN1 and other proteins of cytoskeleton like ankyrin B and glia. All components are crucial for myelin sheath integrity, because in the absence of any of the above loss of axo-glia interaction is observed. The paranodes mainly act as barrier between the nodes with the sodium channels and the juxtaparanodes with the potassium channels. This barrier prevents the passage of nodal currents within the internodes; thus, it is necessary to be formed early during myelination (Yermakov L.M. et. al., 2019).

The third area of myelin organization is the juxtaparanodes. They are part of the internodes and are located adjacent to the paranodes in every myelin structure. The molecular structure of the area consists of CNTN2/TAG-1 located in both axolemma and on glia membrane, the Caspr2 (CNTN-associated protein 2) of the family of neurexins, voltage-gated potassium channels. CNTN2 is crucial for maintaining VGKCs in this area (Traka et al, 2003). For the maintenance of VGKCs at the juxtaparanodes cytoskeleton involvement is required. Precisely, 4.1B a scaffolding protein connects all the aforementioned molecules interacting with VGPCs together with the VGKCs and the cytoskeleton. Ablation of 4.1B together with metalloproteases ADAM22/23 lead to impaired recruitment of VGKCs in the axolemma. These channels characterize the area and are responsible for its functionality as well, due to its potential role, in preventing rapid re-excitation or in preserving the

internodal resting potential (Kalafatakis I. et.al.,2021).

Finally, the internodes are the more extensive domains of the perinodal area. They are myelinated areas right next to the juxtaparanodes and the nodes of Ranvier. The main components of the area are SynCam molecules differently known as members of the Nectin-like family of adhesion molecules and a couple of proteins of immunoglobulin cell adhesion molecules which are critical for the regulation of internodes. These proteins have also the ability to connect to cytoskeleton via FERM-binding domain and a PDZ domain located at the C-terminus with which is probable to bind the 4.1B protein as well (fig.9) (Kalafatakis I. et.al.,2021).

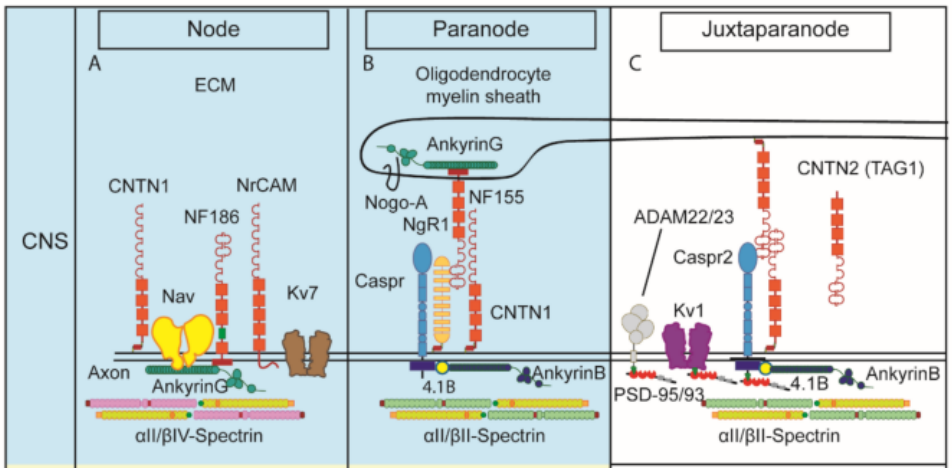

***Figure 9**: Molecular composition of A) the nodes of Ranvier B) Paranodes 3) Juxtaparanodes of the central nervous system (CNS). In each myelin domain are depicted all molecules needed for the formation of compartmentalization of the perinodal area. (Kalafatakis I. et. al.2021)*

1.5 Contactin 2 (CNTN2) or TAG-1

Contactin 2, also known as TAG-1 (Transient axonal glucoprotein-1) and in human as TAX-1, is a protein located at the juxtaparanodes. Just as all proteins belonging to Contactin family, CNTN2 is also composed of several conserved domains like the six immunoglobulin (Ig)-like C2 domains, making these proteins part of the wider immunoglobulin family proteins, four fibronectin III (FNIII) domains and one GPI link domain. As their morphology reveals, contactins are transmembrane proteins but they are also secreted. In the CNS, there are six such proteins, but CNTN1 and 2 are those that we are interested in because they are implicated in the organization of myelinated axons and they interact with plenty molecules both in cis and in trans (fig.10) (Kalafatakis et. al., 2021).

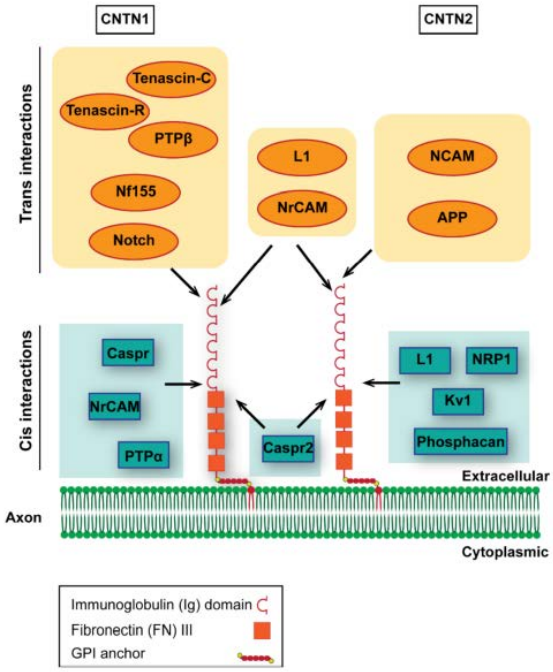

***Figure 10**: Contactins 1 and 2 and their functional domains. Each of the molecules has 6 Ig-C2-like domains which are responsible for their in trans interaction of the molecules with Nf155, L1 and NrCAM, APP and NCAM and in cis with molecules such as Caspr, NrCAM and Li, NPR1 and Kv1. CNTNs carry 4 fibronectin III (FNIII) domains with which mainly interact in cis with Caspr2. Finally, they have a glycosyl-phosphatidyl-inositol (GPI), a domain responsible for their anchoring on the axolemma.*

CNTN 2, is one of the cell adhesion molecules of the juxtaparanodes which apart from the organization of this area, is important in optic nerve structural organization (Chatzopoulou E. et. al., 2008). It is associated with Caspr2 (Contactin associated protein 2) *in cis* and homophilically with glial CNTN2 *in trans* (Traka et al, 2003; Savvaki et al 2010). CNTN2 is expressed in many neuronal subpopulations in different brain areas (cerebral cortex, cerebellum, hippocampus, optic nerve, sciatic nerve etc.) (Kalafatakis et al 2021). It is a protein involved in many processes like the migration of cortical interneurons from ganglionic eminences to their final destinations (Denaxa M. et. al., 2001), neurite extension in both CNS and PNS (Liu Y. Halloran M.C. 2005), in neurogenesis by the interaction of TAG-1 with amyloid precursor protein (APP) via Fe65 adaptor protein in a negative way (Ma Q. H. et al., 2008) and neurite fasciculation (Kunz S. et. al., 1998).

In Cntn2 deficient mice an impaired accumulation of Caspr2 at the juxtaparanodes is observed. In the cuprizone toxic demyelination mouse model, *in vivo*, when TAG-1 is deleted, Kv channels together with 4.1B and ADAM23 have the ability to re-cluster in the juxtaparanodes during re-myelination (Zoupi et. al. 2018). Simultaneously, VGKCs are affected in the absence of CNTN2 in both CNS and PNS and as a result these mice show deficits in learning and memory (Poliak S. et. al., 2003). Additionally, these mice exhibit not only additional behavioral impairment such as affected sensorimotor gating and gait coordination defects but also morphological alterations because they are composed of shorter internodes of the myelinated axons in the cerebral and cerebellar white matter (Savvaki M. et.al., 2008). An important finding that arose from Savvaki M. and colleagues (2010) is that the expression of CNTN2 deriving from glia cells are sufficient for the rescue of

the impaired morphological and behavioral phenotype of CNTN 2 deficient mice.

Apart from *in vivo* studies, clinical ones have shown that both CNTN 1 and 2 are involved in human neurological disorders. Antibodies against CNTN 1 are implicated in peripheral demyelinating neuropathies and against CNTN 2 and Caspr2 in some patients with Multiple Sclerosis (MS). This is an indication that immune response cells directly recognize and interact with the juxtaparanodes in the progression of the disease. Later on, in EAE mouse models, when CNTN2-specific CD4+ T-cells were directly injected in rats, gray matter inflammation was evident to a bigger extent than other models such as MOG-EAE, proposing a precise role of autoimmunity that targets CNTN 2 in gray matter causing inflammation and damage (Derfuss T. et. al., 2009). Although CNTN 2 itself is not associated with any malignancy in human, it is located in the 1q32.1 chromosomal locus, which is strictly corelated to several diseases such as, Usher syndrome type II, malignant gliomas and the Van der Woude syndrome of craniofacial abnormalities (Pieke Dahl S. et. al., 1993; Schröck E. et al., 1994; Sander A. et. al., 1994). In null CNTN 2 knock out mice, deficits in OLs maturation are noticed *in vitro* as well as *in vivo* (Zoupi L. et. al., 2018).

1.4.1 TAG-1 mouse line

CNTN2/TAG-1 is a member of the contactin subgroup belonging to the immunoglobulin (Ig) gene superfamily, as mentioned earler. It is composed of six Ig-like domains of the C2 class and four fibronectin type III-like repeats in its ectodomain while it binds the plasma membrane by a glycosylphosphatidylinositol lipid anchoring domain. Null mutation of TAG-1 by targeted mutation via homologous recombination was reported by F.Fukamauchi et.al, 2001. More precisely, DNA sequence from exon II to exon IV, 5,2kb long DNA fragment, was removed and replaced from neomycin resistance gene (Neo) cassette, 8kb long, while for negative selection diphtheria toxin (DT) was added under the expression of MC1 receptor (Fig.11). The Neo and DT were inserted in the reverse orientation to the TAG-1 gene. Exons II & IV encode the amino acid sequence from the translation initiation site to the first Ig-like domain. With those modifications TAG1 protein, 130KDa, was not detected in TAG1 -/- mice. During crosses scientists ended up to the conclusion that mutant homogenous situation is not lethal because they do not give ratios compatible to lethal situation.

As for the morphology of TAG1 mutant mice, scientists have observed similarities on both size and structure of the CNS between wild type and knock out mice at P2 and E15 on the hippocampus, cerebellum and spinal cord. At the cerebellum, where TAG1 has normally same expression levels to calbindin, a cell specific marker for Purkinje cells, these cells in the

mutant condition were not affected. At the same time, cells, for instance cortical plate neurons and cerebellar granule cells, are not affected by the absence of TAG-1 which in normal condition is a protein highly expressed in those cells. Some TAG1 -/- mice revealed spontaneous epileptic seizures but no overt phenotype was observed in the hippocampus of the TAG-1 -/- mice (F.Fukamauchi et.al, 2001).

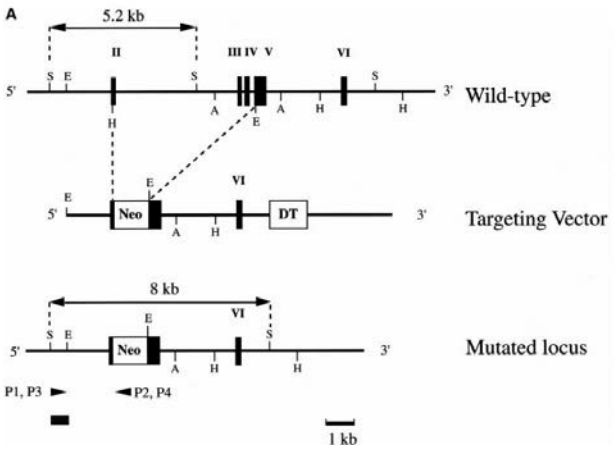

***Figure 11**: Schematic diagram of the strategy used to target TAG-1 gene. Black boxes represent exons for the TAG-1 gene. Translation initiation codon ATG was encoded in exon II. A part of the TAG-1 gene (exons II–V) was replaced with the neomycin resistance gene (Neo). The diphtheria toxin A fragment gene (DT) fragment was ligated at the 3' end of the vector for negative selection. (F.Fukamauchi et.al, 2001)*

2. Materials and Methods

2.1 Animals

All animals in this study were Agouti weighing 15-30 g depending on the developmental stage. Animals were kept in the animal facility of IMBB FORTH under standard conditions in a temperature-controlled facility on a 12 hr light/dark cycle, fed by standard chow diet and water ad libitum with free access to food and water. The animal experiments were carried out according to the National Institutes of Health guidelines for the care and use of laboratory animals and the facility (license nos. EL91-BIObr-01 and EL91-BIOexp-02) complies with all regulations and standards outlined in the Presidential Decree 56/30.04.2013 (Greek Law).

2.2 DNA extraction & Genotyping

Mouse samples were collected and centrifuged at 12.000 rcf for a minute. Equal volumes of NaOH (50mM) and EDTA (0,4M) were added and the samples were placed at 95^{o}C for at least an hour. In the meanwhile, samples were vortexed constantly every 20 minutes. The reaction was neutralized with the addition of Tris pH=8.0.

For the genotyping 3 primers (TAG1.5'-2: GCTCTACAGCCCAGGCAGTTC, length: 21bp, TAG1.3': CTTTGCCACATTGTGCTGTG length:20bp, Neo.3': GAAGACAATAGCAGGCATGC) were used for the identification of TAG1 gene. More precisely, primer TAG1.5'-2 together with TAG1.3' reflect the WT situation (PCR product: 459bp), while primers TAG1.5'-2 and Neo.3' imprint the DEFICIENT one (PCR product: 200bp). Also, we used the following pair of primers Forward primer (F') : 5'-CCATGGATCCTGATGATGTTGTTG- 3' and as Reverse primer (R) 5'-GAATTCTCACAAAGATCGCCTGACACG -3' for the identification of Diphtheria Toxin A (DT-A) (F.Fukamauchi et.al, 2001).

TAG1	Concentration	Volume
Genomic DNA	-	2 μl
Buffer (Enzyquest)	1x	2 μl
dNTPs	2mM	2 μl
TAG1.5'-2 primer	10pmol/ μl	1 μl
TAG1.3'	10pmol/ μl	1 μl
Neo.3'	10pmol/ μl	1 μl
Taq Polymerase	2,5units/ μl	0,7 μl
ddH_2O		10,3 μl

DT-A	Concentration	Volume
Genomic DNA	-	2 μl
Buffer (Enzyquest)	1x	2 μl
dNTPs	2mM	2 μl
DTA F'	100ng/ μl	0,2 μl
DTA R'	100ng/ μl	0,2 μl
Taq Polymerase	2,5units/ μl	0,4μl
ddH_2O		13,2 μl

PCR Conditions		
TAG1	**Temperature**	**Time**
Denaturation	95°C	3min
Denaturation	95°C	30sec
Annealing	60°C	30sec
Extension	72°C	1min
Final Extension	72°C	5min
Hold	4°C	forever

PCR Conditions		
DT-A	**Temperature**	**Time**
Denaturation	95°C	3min
Denaturation	95°C	30sec
Annealing	59°C	30sec
Extension	72°C	1min
Final Extension	72°C	5min
Hold	4°C	forever

2.3 Tissue fixation, isolation, cryoprotection

Twenty-two days old mice receive intraperitoneal injection of euthanasia composed of Ketamine and Xylazine in a ratio of 40-30 accordingly. For adult mice the appropriate volume is 70-80µl but for juvenile (around P20) 50µl. Experimental mice transcardially perfused firstly with cold 1x PBS (Phosphate Buffered Saline) (~20ml), to remove the blood from the tissues through vessels. Blood, complicates the imaging by enhancing false positive signal (background) and also can inhibits proper fixation of brain due to vascular semi-permeability to fixative. Secondly, animals receive 4% Paraformaldehyde (PFA)(~15ml), a process known as fixation, diluted in 1x PBS. Shortly after perfusion has finished, brain tissues are dissected carefully and placed in 4%PFA at 4^{o}C for 30minutes, a process called post fixation, for a better and more complete fixation. Brains were washed tree times in 1x PBS and placed in sucrose 30% with 0.01% NaN3 in 1x PBS for cryoprotection later on.

2.4 Tissue Embedding, Freezing, Cryosectioning

Cryoprotection and more precisely complete intracellular water replacement by sucrose 30%, takes one to two days approximately. Once the brain has been dehydrated, it is embedded in a gel composed of g 15% w/v sucrose, 7.5% gelatin from porcine skin diluted in 1x PBS. Embedded tissue is placed at 4^{o}C for overnight freezing of gelatin. Afterwards, embedded brains when submerged in methyl-butane reach -40^{o}C (up to -35^{o}C) where they are starting to freeze. As soon as the freezing has finished (no observed bubbles), tissue is placed at -80^{o}C for long term storage. Cryosections, is the step that follows freezing during which tissue block is placed in the cryostat where it is necessary to reach -25 ^{o}C. Then the block is cut in sections at different thickness width. More precisely, for cell counting I had used 20µm thick sections, during co-localization experiments 10µm, while for LPC experiments 14µm. Sections were collected on subbed normal slides (not superfrost) and stored at -20^{o}C until further processing.

2.5 Immunohistochemistry on cryosections

After reaching room temperature, cryosections are encircled with DACO PEN, a hydrophobic pen for slides in order to avoid buffer leakage. Then, they are post-fixed in acetone at -20^{o}C for strictly 10minutes. After post-fixation, they are washed three times with 1x PBS for 10 minutes. Then, they are incubated with blocking buffer composed of 5%

BSA(Bovine Serum Albumin, A1391, AppliChem), 0,5% Triton-100X in 1x PBS for an hour at room temperature in a dark place. When the time passes, blocking buffer is removed and slides are incubated with the appropriate primary antibodies diluted in blocking buffer and they are placed at 4^{o}C for 16-18hours (overnight). Cryosections are next washed three times in 1xPBS with 0,1%Triton for 10 minutes. Afterwards, they are incubated with secondary antibodies (usual dilution 1/800) tagged with fluorescent label in blocking solution for two hours at room temperature in dark. Finally, for nuclear signage, it is usually used TOPRO, so, slides after secondary antibody are washed once in 1xPBS for 5 minutes and then are incubated with TOPRO 1/2000 diluted in 1x PBS at room temperature for two minutes. For DAPI (1/1000 or 1/2000), instead, it is always added together with secondary antibodies. To finish immunohistochemistry, it is important to wash three times with 1xPBS with or without triton and put the mounting medium (Mowiol) together with a coverslip to protect and facilitate imaging in Confocal microscopy (Leica sp8 DMi8, Confocal microscopy). Once the mounting medium has been stabilized it is important to encircle coverslip with polish for long term storage of slides at 4^{o}C.

List of secondary antibodies -fluorescent conjugated probes			
Antibody	Animal	Company	Dilution
a-Rabbit IgG-Cy3	goat	Jackson ImmunoResearch Laboratories(#111-165-003)	1/800

a-Rat IgG-Alexa Fluor 488 or 555, 633	goat	Molecular Probes, Thermo Fisher Scientific/#A11034	1/800
a-Mouse IgG-Alexa Fluor 555	Donkey	Molecular Probes, Thermo Fisher Scientific/#A31570	1/800
a-Mouse IgG-Alexa Fluor 488	Donkey	Biotium /#20014	1/800
a-Chicken IgY-Alexa Fluor 555	Goat	Biotium / #20020	1/2000
a-Rabbit IgG-Alexa Fluor 488	Goat	Molecular probes /#A11034	1/2000
TOPRO /DAPI			1/2000

List of primary antibodies used in the present master thesis

Antibody	Animal	Company/ Code	Dilution
anti-PV	Rabbit	Swant/(Code No. PV 25)	1/2000
anti-MBP	Rat	Serotec/(aa82-87)	1/200
anti-GFAP	Mouse	Sigma-Aldrich/(PrNo.G3893)	1/2000
anti PLP	Rabbit	Abcam/(ab28486)	1/1000
anti- MBP	Chicken	Abcam /(ab123499)	1/1000
anti-Iba1	Rabbit	Waco (019- 19741)	1/500

2.6 Hippocampus dissection

It is an essential procedure for protein extraction. To begin with, after animal sacrifice, to remove the hippocampus from the rest of the brain, we have to follow the subsequent steps.

Place the brain on a cold block, in a direction that the olfactory bulbs are dorsally located and the cerebellum ventrally. With a blade, split the two hemispheres along the mid line. It is feasible to either proceed with each hemisphere in a row or to dissect both of them simultaneously. With the blade carefully remove the cerebellum and the olfactory bulbs. With a spatula, remove the thalamus, the hypothalamus, the fornix, the anterior commissure and the septum. Once the above brain areas have been removed, a half moon-like structure is disclosed close to cerebellum. That is the hippocampus. With the spatula

again, loosen the hippocampus from the rest brain by pushing it towards the cerebral cortex. Finally, cut the connections with the rest of the brain and when all brains have been dissected, freeze them at -80^{o}C.

2.7 Western Blotting

Is a widely used analytical technique to detect specific proteins in a sample of tissue such as extract. Proteins are separated according to their size. Additionally, this method can detect proteins of low concentration because of its high sensitivity.

2.7.1 Tissue preparation

As first step, hippocampal (HPF) tissue has been dissected from wild type (DT-A -; TAG1 +/+) and knock out (DT-A -; TAG1-/-) mice. Then, HPF was incubated in 400 µl RIPA buffer of 10 mM sodium phosphate pH 7.0, 150 mM NaCl, 2 mM EDTA, 50 mM sodium fluoride, 1% NP-40, 1% sodium deoxycholate, and 0.1% SDS, together with protease inhibitor cocktail (PIC) on ice in a ratio of 1:1000. The samples were sonicated at 55Hz one at a time until complete tissual dissolving. A really prominent clue is to keep the temperature of the samples stable at 4^{o}C for protein maintenance. Afterwards, sequential centrifuges were realized to collect the protein extract from the soluble phase, so the first at 12000rpm for half an hour at 4^{o}C, while the rest were performed at 12000rpm at 4^{o}C as well, but for approximately 15 minutes. Centrifuges arrest when no pellet is visible. Discard all pellets but the one of the first centrifuge which represents the insoluble phase which also contains proteins, and store it at -80^{o}C until the end of the process. Protein concentration quantification is as important for a high-quality western blot. For this step Bradford assay (Bio-Rad Laboratories) was performed. It is based on the principle of Coomassie Blue G method. This dye makes blue. complexes with proteins, the intensity of which is measured at 595nm. That intensity is relative to the protein concentration in the sample. For this method it is used 790µl ddH_2O, 200µl Bradford and 1-10µl sample and then, the timer is set at 10min. When the time passes, the sample is transferred in cuvettes and their Optical density (OD) was measured at 595nm. As blank is used RIPA with protease inhibitor cocktail (PIC), of equal volume with the tissue sample for calibration while the concentration was standardized with the aid of BSA curve. Once protein concentration is measured, sample is aliquoted and placed at -80^{o}C for long term storage while in the sample loaded in SDS-PAGE add the appropriate amount of 4x Loading buffer of 12ml Tris-HCl 0.5M pH 6.8, 12ml Glycerol 100%, 2.4g SDS, 12mg bromophenol blue (approximately – at the edge of a spoon),

to be the ¼ of the total loaded volume. Before loading, add DithioTrietol (DTT) (C_f:0,1M) and boil them at 95^{o}C for strictly 5 minutes for disulfate bonds breaking and protein complete denaturation.

2.7.2 Running

SDS-Polyacrylamide gel is composed of two gels the stacking and the resolving. The former is used to line up the all the protein samples loaded on a gel, so that they enter simultaneously the resolving gel. The latter is to separate the proteins based on their molecular weight. For the Resolving (R) gel mix in sequence the following ingredients: deionized water, Acrylamide/Bisacrylamide 29:1 – stored at 4^{o}C, Resolving Buffer (Tris-HCl 1.5M pH 8.8 + SDS 0.4%) stored at RT, APS 10% (Ammonium Persulfate) stored at -20^{o}C, TEMED (tetramethylenediamine) which acts as a catalyst to APS and accelerates acrylamide polymerization and is stored at 4^{o}C, while for the stacking (S), nanopure water, Acrylamide/Bisacrylamide 29:1, Stacking Buffer (Tris-HCl 1M pH 6.8 + SDS 0.4%) (RT) and APS 10% (Ammonium Persulfate) and TEMED. When all components are added in the mix for resolving buffer, isopropanol is used for sealing R gel from oxygen and for bubble removal. After its polymerization isopropanol is removed and stacking gel is taking its place. When polymerized, the gel is ready for sample running. Equal volumes of total protein were added in SDS-Polyacrylamide gel of various acrylamide concentration (8-14%). For 1L 1x Running buffer use Tris-base (Cf=25mM) 3.03gr, Glycine for molecular biology (Cf=192mM) 14.4gr and SDS (Cf=0,1%) 1 gr. The running was realized at firstly at 70V until proteins reach the edges of stacking with resolving gel and secondly at 90V when proteins enter the resolving gel, the duration is strictly correlated to acrylamide concentration. **For example**: for 14% gel use→ ddH2O 1,9ml, acrylamide/bisacrylamide 29:1 3,5ml, Resolving buffer 1,95ml, APS 70µl, TEMED 3,3-4 µl in total ~7,5ml.

2.7.3 Transfer

For the transfer, it is needed 1L of 1x cold Transfer buffer which has the same components as running buffer (apart from SDS), plus methanol 20%. Methanol promotes dissociation of SDS from the protein and improves absorption of proteins into membranes in the presence of SDS. For a successful transfer it is crucial to prepare correctly the sandwich/stack of all parts. More precisely, all components are placed with the following sequence, **black** (refers to electrodes, anode), **black** (the plastic face of the plastic surface that retains sandwich structure), **sponge**, **2x Wattman paper**, **gel**, **membrane**, **2x Wattman paper**, **sponge**, **white**

(the other plastic face of the plastic surface), **red** (refers to electrodes, cathode). Nitrocellulose membrane had been used while the transfer is realized at 320mA for an hour. The time required for transfer depends on the molecular weight of each protein. Proteins with higher Mr need more time to be transferred compared to others with a lower one. For example, for a protein <70kDa transfer lasts for an hour at 320mA, for a protein in between 70-110kDa, 1 ½ hours at 320mA and for one over 110kDa, 2 hours at 320mA. After transfer, add Ponceau stain (RT) in a tray. You should see the proteins and the ladder bands. Mark with a pencil the bands of the ladder, the up and down part of the membrane (2 and 3 dots - with 3 dots mark the desired bands). With scissors, cut the membrane according to your needs or leave it as it is. Afterwards, return the stain in its bottle and wash with PBS Tween 0.1%, enough to remove Ponceau. It is an optional step but really important, to check if samples are equally loaded and protein concentration as well.

2.7.4 Immunoblot & Imaging/ Detection

Before immunoblotting, blocking is essential to cover all potential specific or general epitopes of nitrocellulose membrane. In a tray of our choice the membrane is placed and blocking buffer composed of 3% BSA (Applichem, #A1391) in PBST (tween 0.1%) is added. Membrane is incubated for 1h on the shaker at RT or O/N at 4^{o}C. Afterwards, the combination of the first Abs is diluted in the blocking buffer and membrane is incubated for overnight at 4^{o}C. The amount of buffer used is usually up to 3ml, and membrane is wrapped in gelatin with sealed edges. Washes occur trice later on with 1xPBS and 0,1% Tween-20 for 10minutes each.

List of primary Abs used for Western Blotting

For the observation is important to use secondary antibodies conjugated to horseradish peroxidase (HRP) enzyme, which were incubated with nitrocellulose membrane for severely an hour at room temperature. When the time passes, wash three times with 0,1% Tween-20 in 1xPBS. For imaging, horseradish peroxidase (HRP) reacts with HRP substrate luminol and emits light at 428nm which can be detected by a digital manager or on an X-ray film. The emission of light is weak so enhancers are used to increase the signal. This enhancement is known as enhanced chemiluminescence (ECL). The light of the above reaction was detected by ChemiDoc XRS+ BioRad whereas the intensity of the bands was further analyzed with FIJI image J software.

Antibody	Animal	Company/Code	Dilution
anti-PLP	Rabbit	Abcam	1/1000
anti-MBP	Rat	Serotec	1/2500
anti-β-Tubulin	Rabbit	Cell-Signalling Technology (2146S)	1/1000
List of secondary Abs used for Western Blotting			
Anti-Rabbit HRP (Horseradish peroxidase fused with secondary rabbit Ab)	Goat	Merk(#AP132P)	1/4000
Anti-Rat HRP	Donkey	Merk (#AP189P)	1/10.000

2.8 Lysophosphatidylcholine (LPC) injection

During our study it was used LPC demyelinating mouse model to study both demyelination and remyelination on Parvalbumin positive Interneurons located on the hippocampus CA1 region. For focal demyelination induction with LPC injection we followed the protocol from Ferent et al. 2013 but as for the coordinates, we used Mouse Brain Atlas for their determination. Our first set of coordinates that target str. Radiatum (fig.13) of CA1 was Anterior/Posterior (**A/P**) -0.22cm, Medial/Lateral (**M/L**) -0.20cm, Dorsal/Ventral (**D/V**) -0,18cm from dura. As for the process of focal demyelination, Agouti mice were used of over 8 weeks old, weighted and received the proper amount of anesthesia of Ketamine-Xylazine (per gr of animal :100μg of Ket and 15μg of xyl)- Vehicle (1x PBS sterile) intra-peritoneally in a ratio of 1,5-1-4,5. Before the experimental process, mice were checked for pain responsiveness by pinching the tail or the hind limb. Each mouse was stabilized on a small animal stereotactic frame by means of a mouse nose clamp adaptor and ear bars (fig.12) which are incorporated on the frame. The head was positioned so as to assure that the height of the bregma and

lambda was identical, as well as that of the right and left hemisphere. The skull was exposed with the aid of a scalpel and a drill was used to create a small opening. Then 1μl of LPC of 1,25% LPC w/v diluted in 1x sterile PBS from Sigma-Aldrich was injected in a flow of 0,1μl/min. Next, animals were carefully removed from the frame, sutured and left to recover in a clean cage with excess of food and water. Mice were grouped by two (fig. 14).

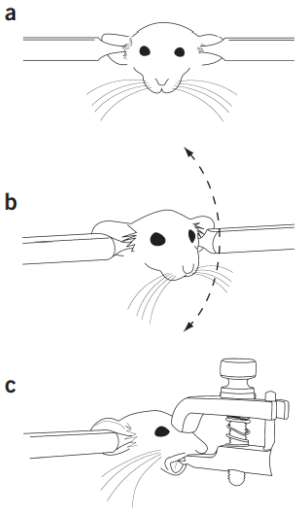

***Figure12**: Proper positioning and fixation of mouse head. (a,b,c) three different angles. (a,b) Immobilizationwith ear bars, so the head has to be symmetrically positioned. (b) dotty line represents the nose movement. Although the mouse is stabilized, the nose is flexible enough to move up and down. (c) The mouth is further stabilized with the aid of the incisor adapter, in a way that the tongue does not cause breathing difficulties to the mouse. Finally, the nose clamp is carefully tightened. Cetin A. et al., 2007*

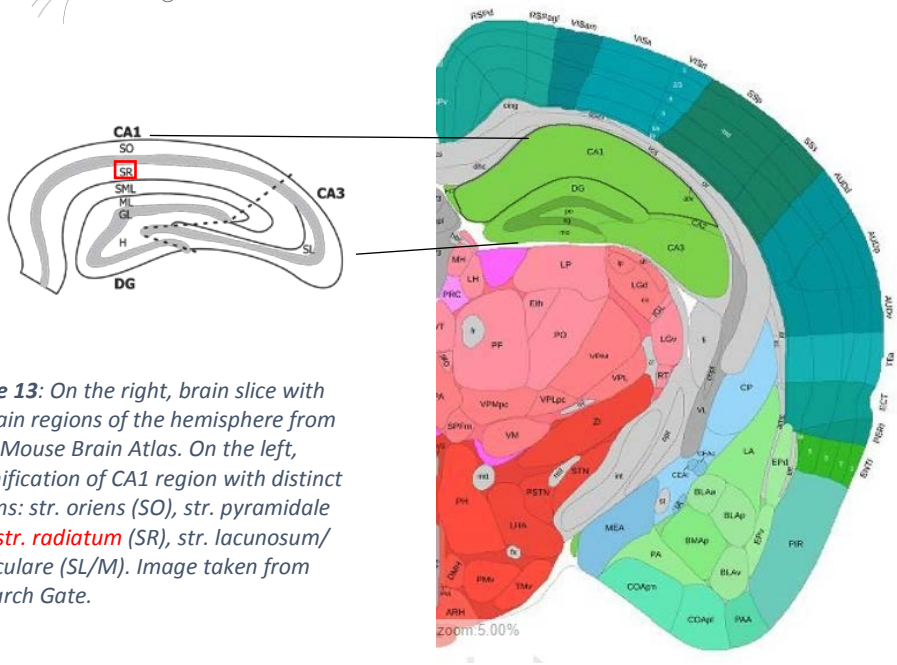

***Figure 13**: On the right, brain slice with all brain regions of the hemisphere from Allen Mouse Brain Atlas. On the left, magnification of CA1 region with distinct regions: str. oriens (SO), str. pyramidale (SP), str. radiatum (SR), str. lacunosum/ moleculare (SL/M). Image taken from Research Gate.*

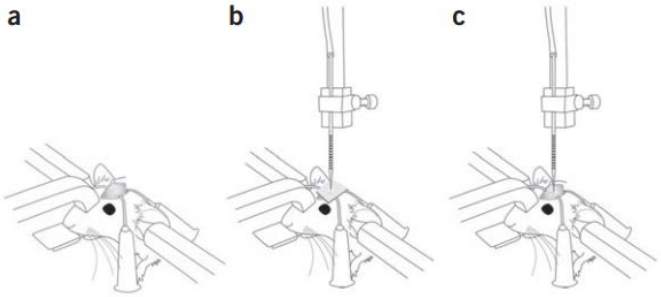

***Figure 14**: Surgery and LPC delivery. (a) With a scalpel open a small wound on the skull, which is kept hydrated with vehicle (0,9% NaOH) and opened. (b) define the bregma and mark the proper position where drilling is about to originate. (c) drill gently the skull and re-define the co-ordinates (x,y,z), then LPC is injected with the aid of the Hamilton pipette. The speed and volume are determined from a device located approximately to the stereotactic device. Cetin A. et al., 2007*

2.8 Electron Microscopy (EM) sample preparation

2.8.1 Animal Perfusion

The fixative used for perfusion is composed of 4% Paraformaldehyde, 15% Picric acid (solution) crucial for antigenicity maintenance and 0.05% glutaraldehyde (GDA) for morphology preservation. GDA is always added is the fixative right before the initiation of the process. For example, for the preparation of 300ml of fixative (final volume), use 12gr of PFA, 45ml of Picric acid, 0,6ml GDA. Firstly, add 95ml ddH_2O in a glass bicker and wait until reaching 60^{o}C, add PFA4%, add ddH_2O up to 105ml and stir, for complete PFA dilution add 2N (approximately 20 drops) NaOH and picric acid. Finally, add 150ml of 0,2M PB (Phosphate Buffer). GDA is always added right before use. Tissue is placed at 4^{o}C for overnight post-fixation in the fixative. For EM experiment 30 days old mice have been used.

2.8.2 Washes

Tissual wash is critical if we want an effective experiment. This is because of picric acid which has to be totally removed from tissue, due to potential inhibition may cause. That is why repetitive washes is 0,1M PB whereas the tissue is shook are realized at 4^{o}C. The duration of washes varies from couple of hours to two days.

2.8.3 Vibratome sections preparation & Tissue cryoprotection

We have used Leica VT1000S vibratome to produce 70μm thick sections. Sections were stored in 0.1M PB, in a well plate (fig.15). Regarding the conditions, I usually use speed around 3 to 4 and frequency 6. These parameters are strongly correlated to the tissue block. If the block is high and its base is small, then the parameters differ from those from a shorter block with the same base. After this step, sections are either stored at 0.1M PB for O/N, or if there is enough time, sections are transferred to washing pots and cryoprotected in sucrose 20%. More precisely, after vibratome sectioning, sections are washed thrice with 1x 0.1PB for 10min at room temperature. Afterwards, sections are incubated in 10% sucrose (made in PB) at room temperature for at least 1hour (1-3 hours). When time passes, 10% sucrose is replaced with 20% for **O/N** incubation at 4^{o}C. Usually, sucrose is freshly made otherwise is stored at -80^{o}C for long term use.

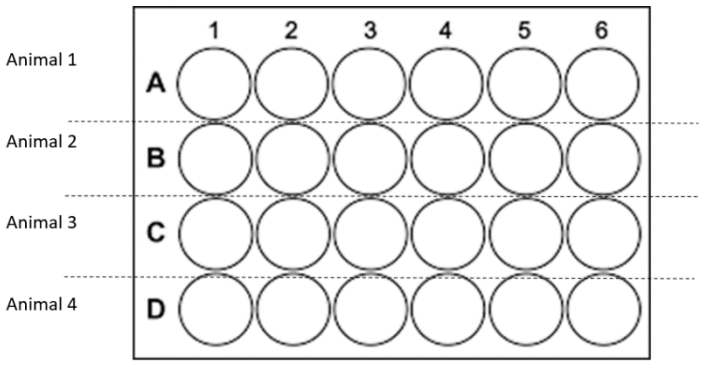

***Figure 15**: 24 well plate used for section storage after vibratome sections preparation. Animals 1 & 2: WT mice and Animals 3 & 4: TAG-1 KO. In each well we have added one section from the appropriate genotype. These are the section that will be subjected to further processing. In our case, we have used sections with dorsal and ventral hippocampus as well.*

2.8.4 Freeze thawing and incubation with the 1st Antibody

After O/N incubation, sections are washed in 20% sucrose just to make sure that the sections have completely been dehydrated. In a 6 well plate all sections are placed from one pot to one well. This step is repeated with sections from all pots. Sections have to be flattened with a brush at the center of the well bottom. Afterwards, excess sucrose is removed from the well. Under the fume hood, the 6 well plate is placed in a tank containing liquid nitrogen. The plate is immersed in the liquid N_2, so deep that the surface where the sections are placed, to be in the nitrogen. Wait until all sections become white. On the working bench, fill up with sucrose 20% and with a brush turn sections upside down. Sucrose is removed and the process with liquid N_2 is repeated one more time. Then, the wells are again filled up in 0.1M PB and the sections are transferred back to washing pots, where is added 0.1M PB. The wash lasts for 5-10 minutes. From now on 50mM TBS (saline buffered with 50mM Tris-HCl, pH 7.4) replaces the 0.1MPB. One wash is realized for 10mins at room temperature. Sections then are incubated with 20% NGS (Normal Goat Serum, Ci=100%) for at least 1 to 2 hours at room temperature. It serves as blocking solution to cover all non-specific epitopes and is diluted in 50mM TBS. Finally, sections are stored at 4oC for 36 hours (2x O/N) incubation with the first Antibody (Rabbit anti-PV 1/2000, Swant) diluted in 50mM TBS.

2.8.5 Incubation with Secondary Antibody

Two days after the incubation with the first Ab has started, wash three times with 50mM TBS for 10 minutes at room temperature. Incubate the sections with secondary antibody,

(anti-rabbit gold-conjugated Fab', 1/75, Nanoprobes, lot: #24C103), incubate for 36hours (2x O/N).

2.8.6 Silver Enhancement, Processing with Osmium/Uranium, Tissue Embedding

Silver Enhancement (Fig.16)

Sections are washed thrice with 50mM TBS for 10mins at room temperature. Afterwards, 0.5% (from 25%) GDA is prepared in TBS 50mM (V= 1ml for each pot). The sections are incubated in GDA for 10mins at RT, **w/o** shaking for complete immobilization. In the meantime, all components of the silver enhancement aliquots are placed at RT in **dark, because they are light-sensitive** to defrost (HQ SILVER^{TM} Enhancement Kit, Catalog Number: 2012-45ML, Nanoprobes,). Wash once with TBS 50mM and afterwards make consecutively washes with ddH_2O for 5 mins at RT (approximately 4 washes under the fume hood and 3-4 on the bench). Then, sections are flattened at the bottom of the pot. During the last wash, the content from the red-labeled tube (Initiator, colorless solution, low viscosity) is mixed by vortexing with the one from the green-labeled tube (Moderator, pale brown solution, with the higher viscosity of the three) until they become homogenous. The content from blue-labeled tube (Activator: medium viscosity) is consequently transferred and mixed with the other two by vortexing. By the time all components are mixed reaction lasts for **maximum 20mins.** Approximately, 500 µl from the solution is added on the sections, which are then agitated in dark. The sections are observed frequently (every 1-2 min). In 6 to 8 minutes, the sections and the solution have become dark. When time passes, the reaction is stopped by adding ddH_2O. Many parameters can affect the reaction:1) Temperature 2) Tissue quality etc. So, the timepoint that we stop the reaction depends on those parameters. Three washes in ddH_2O at RT are realized, on shaker. By the time, the process is completed the sections have been curved. Then, 50mM TBS is added to restore section shape and curvature. Three washes in 0.1M PB for 5 min are made at room temperature. Buffer exchange is because osmium from the following steps reacts with Tris and precipitation occurs.

Processing with Osmium Tetroxide (OsO_4) And Uranium

After having washed 3x with 0.1M PB, sections are placed in a 12 well plate, because they should be flattened and pressed smoothly to stick on the well's bottom surface. 1.33% OsO4 (500µl) is added on the sections after being diluted in 0.1M PB, and then sections are incubated for 40mins at room temperature under fume hood. Discard OsO4 in the appropriate bottle (placed in the fume hood). 0.1M PB is added and consecutively washes are fulfilled in ddH_2O to remove excess phosphate buffer, because it is precipitated when reacting with Uranium. 1% of Uranium is diluted in ddH2O and well plate with the sections is covered and incubated for 40mins at room temperature in dark.

4% OsO_4	0,2 M PB	0,1MPB
V/3	V/3	V/3

3 x (V/3) = 2000µl

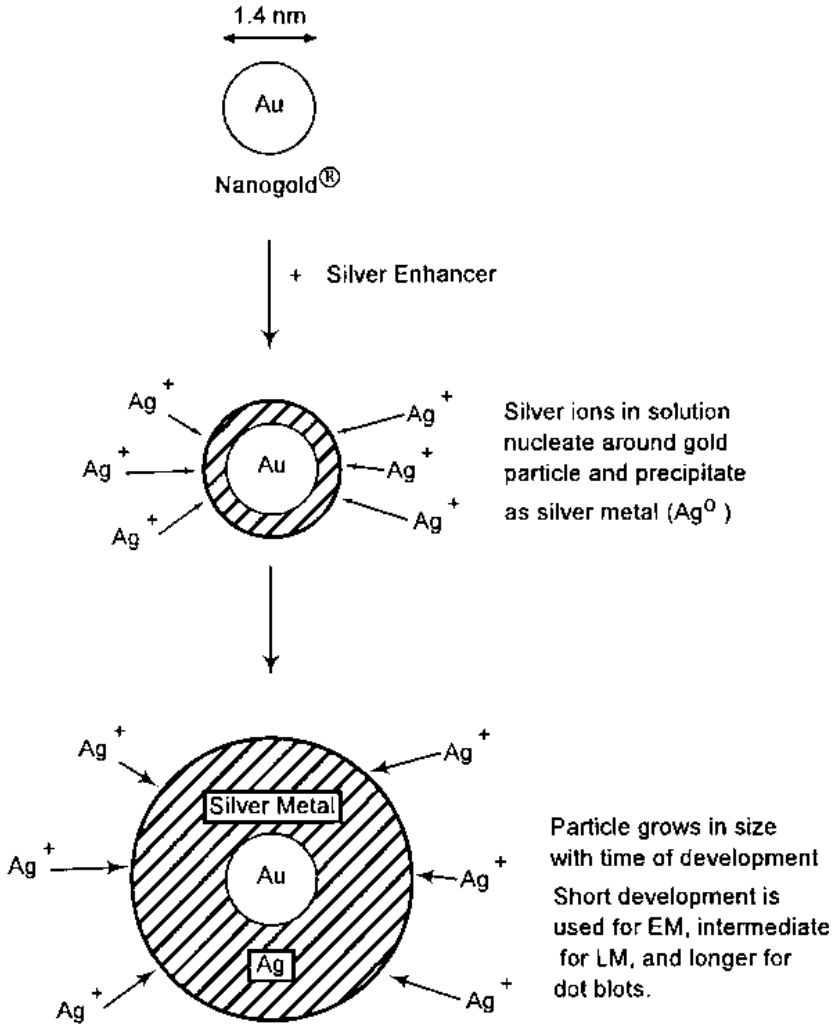

Figure 16: Diagram of silver enhancement process. (Hainfeld J.F & Powel R.D., 2000)

Tissue Dehydration with Alcohol

The sections are washed twice with ddH_2O to remove excess uranium. Water is then replaced with 50% Alcohol two washes are needed, for 5mins each at RT w/o shaking. The same step is repeated with all alcohols (70%, 90%, 95%), when changing from one alcohol to another of higher concentration, the **conditioning** of the pot is necessary. When it is time for 100% alcohol, the incubation lasts for 10 minutes. Finally, 100% EtOH is replaced with propylene oxide (100%, placed under fume hood). In the meanwhile, resin is added in small, plastic tubs where sections are going to be placed as soon as time passes. They are soaked for 2 to 4 hours, until they mire in the bottom surface of the plastic tub. This means that resin has occupied the empty space (water existed before dehydration with EtOH and propylene oxide) of the sections. They are finally placed on the slides and covered with coverslip, which are insulated with pure fat before coverage. O/N incubation at 65^{o}C will induce resin's polymerization. After polymerization, the slides are ready for re-embedding. All steps after O/N polymerization are done whenever we have time. But their logical sequence is the following.

2.8.7 Tissue Re-embedding

For this step it is needed, resin, forceps with curved edges, a scalpel, a toothpick (always use the one with the black), defrost resin and plastic cast, stereoscope- optical microscope and two markers of different colors (red/blue), a razor blade. The cast is cut into 3 pieces (1. Remove the lid, cut the body of the cast up to 2 pieces). With the razor, the coverslips are removed from the slides. Under the optical microscope, the surface that the staining is more intense is marked (In red → top surface, in blue → the bottom one). All slides are placed under stereoscope, with the scalpel and the edges of the tissue area that we want to re-embed are etched. Movements have to be stable and decisive. With the toothpick, a drop of resin on cast's lid is added and the tissue is placed on it with the surface of more intense staining to face the bottom of the lid. The lid is kept at 60^{o}C for 5-10mins. The cast is then filled up with resin and kept again at 60^{o}C for 2-3 mins to remove bubbles. Coverslips are placed on the top of the cast to create a flat surface. Polymerization of resin occurs again after O/N at 60^{o}C. The blocks are given to Professor Y. Dalezios for microsection preparation

and further processing which finally leads to TEM scanning. As for the parameters of the scanning, the voltage we were scanning was at 80KV and the beam current at 45μA.

3. Objective

The aim of the project is to identify the role of myelination in inhibitory neurons of the hippocampus. To further investigate this, we subdivided the project into two main sections: a) the investigation of the role of TAG-1, cell adhesion molecule of the plasma membrane located at the juxtaparanodes, in the hippocampal inhibitory neurons and b) the examination of the vulnerability of inhibitory neurons to demyelination *in vivo*. For the examination of the role of TAG1 in the regulation of hippocampal interneurons, we proceeded to co-localization experiments using confocal microscopy in wild type and TAG-1 deficient animals. Additionally, we examined with ultrastructural analysis of myelin PV interneurons in the two genotypes with Transmission Electron microscopy in conjunction with immunohistochemistry. As for the second part, we proceeded to cause demyelination of the stratum radiatum of the hippocampus with focal injection of Lysophosphatidylcholine (LPC), also known as lysolecithin, a derivative of phosphatidylcholine, known to disrupt myelin lipids in the corpus callosum. The technique in the hippocampus was established as part this work.

4. Results

4.1 Role of TAG-1 in PV interneurons

During this study I analyzed the percentage of axons of PV+ interneurons that are being myelinated in the Cornu Ammonis 1 (CA1) of wild type and TAG-1 deficient mice at the age of p22. Fig.17 shows that there is no statistically significant difference between myelinated segments of PV+ axons of wild type and deficient animals, although in the absence of TAG-1 there are fewer PV+ cells. In this work, three strata have been included, the stratum oriens (str.or), stratum pyramidale (str. pyr), and stratum radiatum (str. rad). It is also obvious that there is a bigger distribution among the deficient animals tested compared to the control ones.

For the measurements, I have used the JACoP from Image J, in which three parameters were selected, Pearson's coefficient, overlap coefficient k1 & k2 and Manders coefficient. Pearson's coefficient, describes the correlation of the intensity distribution

between channels. Overlap coefficient k1 & k2, splits the value of colocalization into two distinct parameters, that allow to determine the contribution of each one to the areas with co-localization. Finally, Mander's coefficient shows a real overlap of the signals, so it represents the true degree of colocalization (Zinchuk V. et al 2007). Samples were analyzed with the aid of Threshold.

To further quantify the myelin found in wt and TAG1 deficient hippocampus, I proceeded to western blot analysis. For this , I used antibodies for MBP (Myelin Basic Protein) and PLP (Proteolipid Protein), two of its main myelin structural components. Western Blotting is also a method that gives the opportunity of quantification of protein levels (Fig.18). This analysis has shown that there are no significant alterations between the two genotyes. This finding agrees with the results of the co-localization experiments.

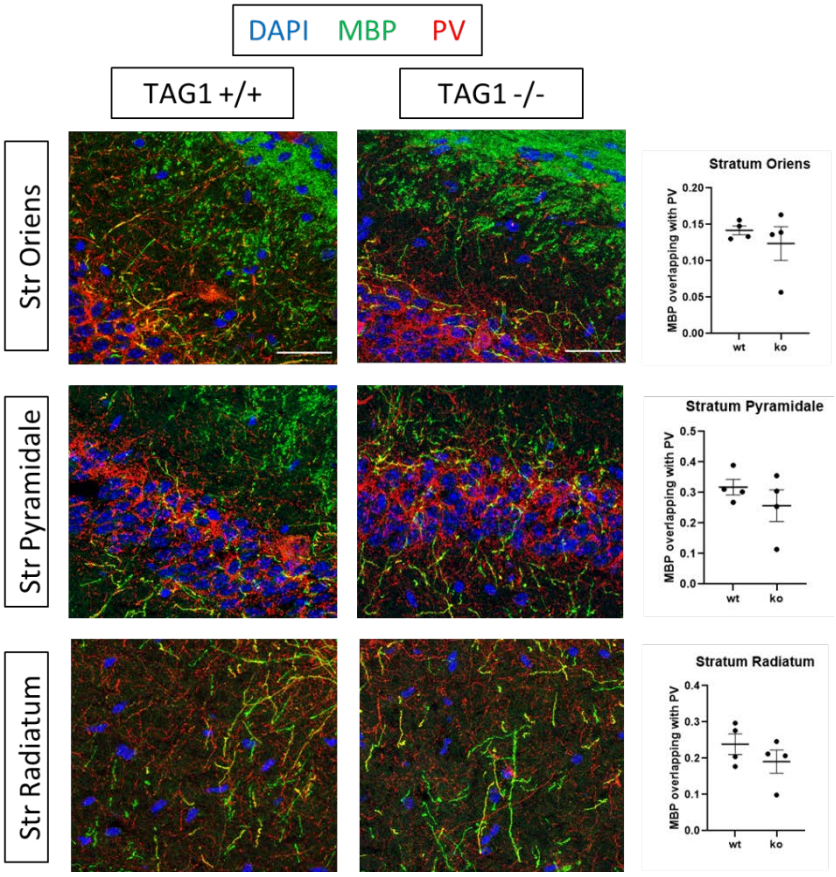

***Figure 17**: Images of the double immunostaining, from stratum oriens, pyramidale, radiatum, of the CA1 region of the hippocampus of wt and TAG1 deficient juvenile mice (p22). In green 10µmthick sections were stained for MBP (Myelin Basic Protein), in red for PV (interneuronal subtype) and in blue, nuclear staining. Scale bar: 30µm. On the right, we have quantifications of the percentage of MBP positive axons overlapping with PV positive ones, in the threehippocampal strata. Animals tested: 4animals/genotype, three*

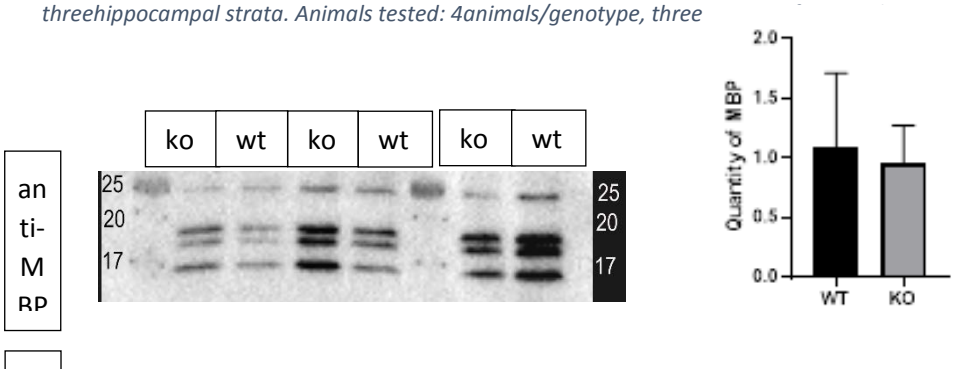

***Figure 18**: Western blotting analysis representing 3 different animals TAG-1 ko and 3 animals wt. Dissection of HPF occured, and protein extract proceed to further processing using antibody for MBP. On the right, a diagram represents the quantity of myelin belonging to HPF of wt and TAG-1ko animals. There is no statistically significant difference between the two genotypes which is in accord with IHC results.*

4.2 Number of Parvalbumin interneurons cells in the hippocampus

Apart from myelin-related alterations in hippocampus due to the ablation of TAG1, we were also interested in examining if any alterations exist in the number of Parvalbumin interneurons in TAG1-deficient animals compared to wt ones. This is because TAG1 is a cell adhesion molecule involved in both neuronal migration and differentiation. I stained for PV cells in 20μm thick brain sections of control and TAG1 deficient animals. Results derive from 3 different sections (anterior, median, posterior) at p22 mice. There is a decrease of the distribution of PV neurons in the hippocampus in the TAG-1 deficient animals. For this result I have tested three animals of the same age, while cells were counted in Fiji software (Fig. 19).

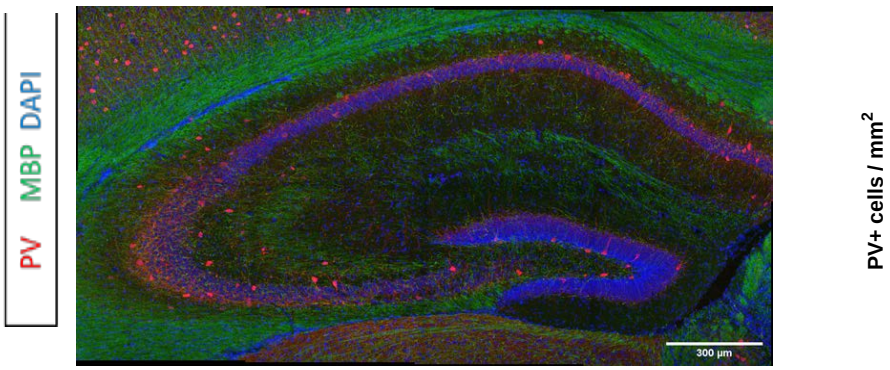

***Figure 19**: On the right, staining of PV interneurons in red (dots), in green MBP and nuclear staining on blue. It is an indicative image from an TAG1 deficient mouse at p22. On the left, diagram showing the number of PV per area (y axis) and the genotype of the animals tested (x axis). For the calculations t test was performed and 3 animals were tested (3 sections of 20μm per animal).*

4.3 Myelin morphology of PV interneurons in Tag1 deficient animals

Although TAG-1 deficient animals did not reveal any significant decrease in myelin percentage belonging to PV cells, we wanted to further analyze the level of the impact myelin might have in the two genotypes. For this reason, we proceeded to ultrastructural analysis using Transmission Electron Microscopy (TEM) which enables us to image myelin at significantly higher resolution comparing to light microscopy. We proceeded to perform immunohistochemistry for Electron microscopy (Immuno-EM) and below axons are depicted belonging to wild type animals and TAG-1 deficient ones. Also, we measured the g ratio of myelin which is defined as the ratio between the inner axon radius and the outer radius of myelinated axons. It is a parameter characteristic of every axon that changes upon myelin alteration.

For the staining of PV interneurons, we used antibodies against Parvalbumin (Rabbit anti-PV) from Swant in a dilution 1:2000. For the secondary antibody we used Gold anti-Rabbit from Nanoprobes in a ratio of 1:75. For g ratio diagram, I analyzed 48 myelinated axons from wild type animals and 32 from TAG-1 deficient ones. The g-ratio does not differ between the two conditions but we need at least 100 axons from each genotype to come to a conclusion (Fig.20). Therefore this experiment is still in progress.

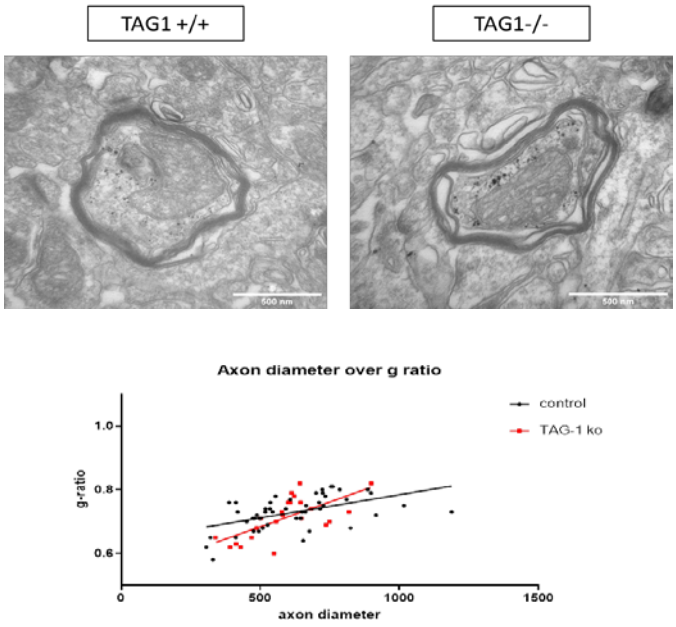

Figure 20: *Ultrastructural analysis of PV interneurons of str. radiatum from TAG1 deficient mice and wt at p30. Immuno EM, for PV interneurons labeled with Ab fused with Gold, shows alterations in the morphology of myelin in TAG1ko background of p30 mice. B. G-ratio diagram of 48 wt axons and 32 TAG-1 ko. Scale bar: 500nm*

4.4 Vulnerability of PV axons to demyelination

Generally, there are three models used, to provoke demyelination: genetic, pathogen induced and toxin-related. In this study we have chosen the third type of demyelination, where focal injection of Lysophosphatidilcholine (LPC) (or Lysolecithin) is performed in adult mice (p70-80). It is one of the two main toxin-mediated models which lead to focal demyelination. It is a method where the outcome is immune system-independent (Miller R. H. et al., 2010). LPC, when injected into the area of interest and due to its direct action, leads to myelin impairment (Lassmann H. et al., 2017; Blakemore W. F. et al., 2008). It initiates toxicity by integrating into cellular membranes and leading to both cell death and demyelination later on (Plemel J. R. et al., 2017). Simultaneously, it attracts the monocytes that trigger immune response in the affected area. After demyelination, spontaneous remyelination occurs the moment when all myelin debris have been removed and lasts for weeks. In the case of LPC injection, it starts approximately 10-15 days after injection (Hall S. M. 1979). The method is extensively used for demyelination studies of the corpus callosum and I had to adapt it for the hippocampus as discussed below.

To conduct focal demyelination, it is important to use the appropriate coordinates to reach the hippocampus and more precisely the stratum radiatum. This step was the most challenging due to the fact that few scientific works have been published regarding this model in the mouse. Some have been performed in the rat hippocampus instead. The coordinates used were standardized by mouse brain atlas and by small modifications depending on the results. Agouti adult mice were received 1µl of 1,25%w/v LPC (diluted in 1x PBS sterile) in a flow of 0,1µm/min. Seven days after the injection mice were sacrificed. Below is depicted immunohistochemistry of 14µm thick sections stained for MBP (in green) and TOPRO(in blue) and for microglia or astrocytes which further validate the presence of LPC and demyelination within the area of interest. Although, microglia staining is an important step of lesion determination, nuclear staining is also capable to determine this area. As observed in Fig. 21 in the case of LPC injection de-myelination exists if we compare with the equivalent area of the brain injected with PBS which has no significant alteration.

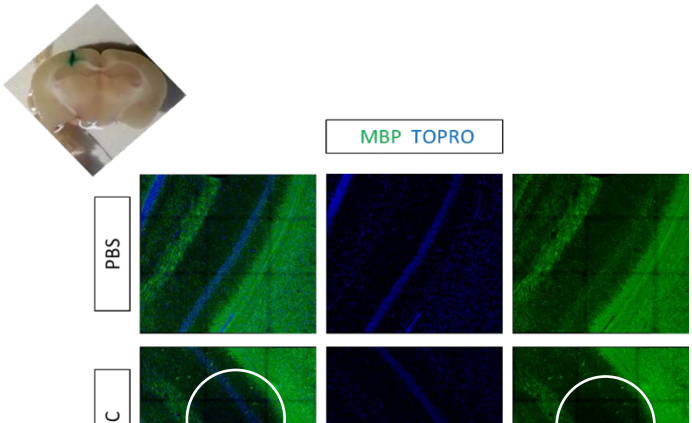

Figure 21: *Stereotactic injection of LPC into str Radiatum of CA1. At day 0 adult mice were injected with LPC 1,25% at str. rad. They were sacrificed at day 7. In the upper line the mouse received 1x sterile PBS, which is the solution LPC is diluted and serves as control. The bottom line depicts IHC for MBP at the CA1. Marked area indicates the position of impaired*

5. Discussion

Inhibitory neurons regulate the excitation and inhibition balance among neurons and accordingly, prevent over-excitability and excitotoxicity. Micheva K. D. and colleagues have recently found that PV interneurons are heavily myelinated in the cortex. A slew of other works not only confirmed this but also found that many hippocampal interneurons are not only myelinated but also express a great number of Kv.1 channels. Kv1 channels are aggregated at the juxtaparanodes, anchored in scaffolding proteins and neighboring with other proteins related to cell adhesion molecules (CAMs). One of such proteins is the TAG-1, also known as Contactin 2 (CNTN2), located at the juxtaparanodes and responsible for the proper positioning of Caspr2 along the distal axon.

To investigate the significance of TAG-1 in PV interneurons of the CA1 hippocampal area, we used TAG-1 deficient and wild type mice of 22 days of age. By performing immunohistochemistry for PV interneurons and for MBP as a myelin marker, we measured the levels of MBP in these interneurons in the absence of TAG-1 and in control mice. Our findings (fig 15.) indicate that there is no statistically significant difference between wild type and TAG-1 deficient mice, but in the case of str. radiatum the values deriving from TAG-1 deficient mice tend to be reduced when compared to wild type ones. This is possibly due to the fact that the axons of PV interneurons extend in the str. Radiatum. Alternatively TAG-1 is not essential for myelin formation, but for the organization of myelin fibers by maintaining the cohesion of the juxtaparanodal area. To further investigate this, we proceeded to Western blotting analysis using hippocampal formation (HPF) from TAG-1 deficient mice and wild type at p22. The quantification affirms the results from co-localization analysis. These findings may indicate that either TAG-1 is not a crucial component for myelination of PV interneurons at this developmental stage, when myelination has not been fully completed yet. Therefore, older mice could be examined, at 2 months of age. Definitely we have to ensure that myelination maintenance is not impaired. For this experiment we must analyze myelination in adult mice as well. It is also important to investigate the quality of myelin in the two genotypes in the hippocampus.

To test whether myelin quality of PV interneurons is affected, we proceed to ultrastructural analysis using Transmission Electron microscopy (fig.18). For this experiment we realized immunohistochemistry for PV interneurons but this time for electron microscopy. As myelin quality, I am referring to proper filament formation and accordingly their wrapping along axons and myelin geometry (thickness, compaction, sheath number and sheath length).

We studied myelin thickness by determining the g-ratio. As already mentioned, g-ratio is defined as the ratio between the inner and the outer axon radius of myelinated axons. G-ratio diagram of 48 wild type and 32 TAG-1 deficient axons was prepared. As shown on the g-ratio diagram no significant difference is depicted but there are differences between the genotypes. Since the work is still in progress, more axons will be counted to come to a conclusion. Furthermore, it is important to test if other parameters of myelin geometry are altered, because TAG-1 is component of myelinated neuronal axon and of oligodendrocytes as well. It is yet worthy to check whether TAG-1 impair proper myelin deposition. Thus, it is important to analyze the morphology of myelin sheath in addition to the g ratio, work that is currently in progress. Additionally, quantification of axons according to their diameter, may differ, so it is a parameter that has to be tested. According to earlier reports (Chatzopoulou E. et. al., 2008), we are expecting to have a decrease in the myelin thickness or of other parameters such as myelin lamellae, microtubuls/neurofilaments.

Additionally, we counted the total number of PV cells located at the hippocampal formation (HPF). We took advantage of the already existent immunohistochemistry experiment, for PV interneurons and for MBP and we observed that the number of PV interneurons tends to be reduced in TAG-1 deficient background comparing to control mice. At least, two more animals must be analyzed to come to a more valid conclusion because of the high distribution of the values that have already been analyzed. Apart from the total number of PV cells in the HPF, we have to count their number in each CA subdomain, or among strata of the CA sub-compartments independently. If their number is decreased it is possible that the absence of TAG-1 impairs their migration or even generation (Denaxa M. et. al., 2001; Kunz et. al., 1998; Liu & Halloran, 2005), and accordingly their function. It could also be that the absence of TAG-1 impairs their myelination so apoptosis occurs due to potential abolishment of axon potential propagation or metabolic support provided by oligodendrocytes (OLs). An explanation to how possible is to have a decrease number of PV positive cells and a kind of normal myelin quantity belonging to such interneurons in TAG-1 deficient mice, is because the remaining PV myelinated cells could produce more branches

that can rescue the intending damage.

To test if PV positive interneurons are vulnerable to demyelination and also to examine their intrinsic characteristics and synaptic inputs as well, after de-myelination and remyelination it is important to cause demyelination. There are a couple of methods used for demyelination but two of them are widely used. The first one is the cuprizone model, in which toxin is included in animal's diet and causes systemic demyelination and the second the lysolecithin (LPC) injection within the brain area of interest causing focal de-myelination. We have chosen the second type that causes limited demyelination in the area injection was performed. For this experiment, it was necessary to use the appropriate co-ordinates. After repeated trials, as indicated at fig.19, we have succeeded to reach the str. radiatum of the CA1 hippocampal area, but there is no nuclear accumulation in the area of de-myelination. In the literature it is widely acknowledged that LPC induces microglia and accordingly, inflammation in the targeted area. This is most likely due to experimental handling, or to particularity of the hippocampal area which is full of astrocytes and other microglia in normal conditions.

Myelination of interneurons is a highly active scientific area especially recently. In the past, interneurons were thought not to be myelinated, an opinion confuted with the scientific work of Micheva and colleagues. With our attempt we are trying to shed light in the myelin organization and the importance of cell adhesion molecules such as CNTN-2/ TAG-1 that PV and SST interneurons carry on their axons (Bonetto G. et. al, 2019). TAG-1 is a glycoprotein that is implicated either implicitly or explicitly in neurological diseases like MS, while PV interneurons and oligodendrocytes were altered in neurodevelopmental disorders like schizophrenia. PV interneurons and OLs apart from common origin and transcriptional similarities seem to have a more substantial relationship that remain to be elucidated (Benamer N. et. al., 2020). The hypothesis is being put forward that dysregulation of their intimate relationship may be implicated in schizophrenia (Benamer N. et. al., 2020).

6. Reference

Amaral, D. G., & Witter, M. P. (1989). The three-dimensional organization of the hippocampal formation: a review of anatomical data. *Neuroscience, 31*(3), 571-591. doi:10.1016/0306-4522(89)90424-7

Balia, M., Benamer, N., & Angulo, M. C. (2017). A specific GABAergic synapse onto oligodendrocyte precursors does not regulate cortical oligodendrogenesis. *Glia, 65*(11), 1821-1832. doi:10.1002/glia.23197

Bechler, M. E., Byrne, L., & Ffrench-Constant, C. (2015). CNS Myelin Sheath Lengths Are an Intrinsic Property of Oligodendrocytes. *Curr Biol, 25*(18), 2411-2416. doi:10.1016/j.cub.2015.07.056

Bechler, M. E., Swire, M., & Ffrench-Constant, C. (2018). Intrinsic and adaptive myelination-A sequential mechanism for smart wiring in the brain. *Dev Neurobiol, 78*(2), 68-79. doi:10.1002/dneu.22518

Benamer, N., Vidal, M., & Angulo, M. C. (2020). The cerebral cortex is a substrate of multiple interactions between GABAergic interneurons and oligodendrocyte lineage cells. *Neurosci Lett, 715*, 134615. doi:10.1016/j.neulet.2019.134615

Bezaire, M. J., & Soltesz, I. (2013). Quantitative assessment of CA1 local circuits: knowledge base for interneuron-pyramidal cell connectivity. *Hippocampus, 23*(9), 751-785. doi:10.1002/hipo.22141

Bjorefeldt, A., Wasling, P., Zetterberg, H., & Hanse, E. (2016). Neuromodulation of fast-spiking and non-fast-spiking hippocampal CA1 interneurons by human cerebrospinal fluid. *J Physiol, 594*(4), 937-952. doi:10.1113/jp271553

Blakemore, W. F., & Franklin, R. J. (2008). Remyelination in experimental models of toxin-induced demyelination. *Curr Top Microbiol Immunol, 318*, 193-212. doi:10.1007/978-3-540-73677-6_8

Bliss, T. (2007). *The hippocampus book*. New York, NY, US: Oxford University Press.

Bonetto, G., Hivert, B., Goutebroze, L., Karagogeos, D., Crépel, V., & Faivre-Sarrailh, C. (2019). Selective Axonal Expression of the Kv1 Channel Complex in Pre-myelinated GABAergic Hippocampal Neurons. *13*(222). doi:10.3389/fncel.2019.00222

Booker, S. A., & Vida, I. (2018). Morphological diversity and connectivity of hippocampal interneurons. *Cell Tissue Res, 373*(3), 619-641. doi:10.1007/s00441-018-2882-2

Caillard, O., Moreno, H., Schwaller, B., Llano, I., Celio, M. R., & Marty, A. (2000). Role of the calcium-binding protein parvalbumin in short-term synaptic plasticity. *Proc Natl Acad Sci U S A, 97*(24), 13372-13377. doi:10.1073/pnas.230362997

Cetin, A., Komai, S., Eliava, M., Seeburg, P. H., & Osten, P. (2006). Stereotaxic gene delivery in the rodent brain. *Nat Protoc, 1*(6), 3166-3173. doi:10.1038/nprot.2006.450

Chatzopoulou, E., Miguez, A., Savvaki, M., Levasseur, G., Muzerelle, A., Muriel, M. P., . . . Thomas, J. L. (2008). Structural requirement of TAG-1 for retinal ganglion cell axons and myelin in the mouse optic nerve. *J Neurosci, 28*(30), 7624-7636. doi:10.1523/jneurosci.1103-08.2008

Denaxa, M., Chan, C. H., Schachner, M., Parnavelas, J. G., & Karagogeos, D. (2001). The adhesion molecule TAG-1 mediates the migration of cortical interneurons from the ganglionic eminence along the corticofugal fiber system. *Development, 128*(22), 4635-4644.

Derfuss, T., Parikh, K., Velhin, S., Braun, M., Mathey, E., Krumbholz, M., . . . Meinl, E. (2009). Contactin-2/TAG-1-directed autoimmunity is identified in multiple sclerosis patients and mediates gray matter pathology in animals. *Proc Natl Acad Sci U S A, 106*(20), 8302-8307. doi:10.1073/pnas.0901496106

Fields, R. D. (2008). White matter in learning, cognition and psychiatric disorders. *Trends Neurosci, 31*(7), 361-370. doi:10.1016/j.tins.2008.04.001

Ghosh, A., Sherman, D. L., & Brophy, P. J. (2018). The Axonal Cytoskeleton and the Assembly of Nodes of Ranvier. *Neuroscientist, 24*(2), 104-110. doi:10.1177/1073858417710897

Habermacher, C., Angulo, M. C., & Benamer, N. (2019). Glutamate versus GABA in neuron-oligodendroglia communication. *Glia, 67*(11), 2092-2106. doi:10.1002/glia.23618

Habermacher, C., Angulo, M. C., & Benamer, N. (2019). Glutamate versus GABA in neuron-oligodendroglia communication. *Glia, 67*(11), 2092-2106. doi:10.1002/glia.23618
Hainfeld, J. F., & Powell, R. D. (2000). New frontiers in gold labeling. *J Histochem Cytochem, 48*(4), 471-480. doi:10.1177/002215540004800404
Hall, S. M. (1972). The effect of injections of lysophosphatidyl choline into white matter of the adult mouse spinal cord. *J Cell Sci, 10*(2), 535-546.
Hu, H., Gan, J., & Jonas, P. (2014). Interneurons. Fast-spiking, parvalbumin^{+} GABAergic interneurons: from cellular design to microcircuit function. *Science, 345*(6196), 1255263. doi:10.1126/science.1255263
Hu, J. S., Vogt, D., Sandberg, M., & Rubenstein, J. L. (2017). Cortical interneuron development: a tale of time and space. *Development, 144*(21), 3867-3878. doi:10.1242/dev.132852
Huxley, A. F., & Stämpfli, R. (1949). Evidence for saltatory conduction in peripheral myelinated nerve fibres. *J Physiol, 108*(3), 315-339.
Iaccarino, H. F., Singer, A. C., Martorell, A. J., Rudenko, A., Gao, F., Gillingham, T. Z., . . . Tsai, L. H. (2016). Gamma frequency entrainment attenuates amyloid load and modifies microglia. *Nature, 540*(7632), 230-235. doi:10.1038/nature20587
Kalafatakis, I., Savvaki, M., Velona, T., & Karagogeos, D. (2021). Implication of Contactins in Demyelinating Pathologies. *Life (Basel), 11*(1). doi:10.3390/life11010051
Khalaf-Nazzal, R., & Francis, F. (2013). Hippocampal development - old and new findings. *Neuroscience, 248*, 225-242. doi:10.1016/j.neuroscience.2013.05.061
Knierim, J. J. (2015). The hippocampus. *Curr Biol, 25*(23), R1116-1121. doi:10.1016/j.cub.2015.10.049
Konradi, C., Yang, C. K., Zimmerman, E. I., Lohmann, K. M., Gresch, P., Pantazopoulos, H., . . . Heckers, S. (2011). Hippocampal interneurons are abnormal in schizophrenia. *Schizophr Res, 131*(1-3), 165-173. doi:10.1016/j.schres.2011.06.007
Kunz, S., Spirig, M., Ginsburg, C., Buchstaller, A., Berger, P., Lanz, R., . . . Sonderegger, P. (1998). Neurite fasciculation mediated by complexes of axonin-1 and Ng cell adhesion molecule. *J Cell Biol, 143*(6), 1673-1690. doi:10.1083/jcb.143.6.1673
Lassmann, H., & Bradl, M. (2017). Multiple sclerosis: experimental models and reality. *Acta Neuropathol, 133*(2), 223-244. doi:10.1007/s00401-016-1631-4
Lisman, J., Buzsáki, G., Eichenbaum, H., Nadel, L., Ranganath, C., & Redish, A. D. (2017). Viewpoints: how the hippocampus contributes to memory, navigation and cognition. *Nat Neurosci, 20*(11), 1434-1447. doi:10.1038/nn.4661
Liu, Y., & Halloran, M. C. (2005). Central and peripheral axon branches from one neuron are guided differentially by Semaphorin3D and transient axonal glycoprotein-1. *J Neurosci, 25*(45), 10556-10563. doi:10.1523/jneurosci.2710-05.2005
Ma, Q. H., Futagawa, T., Yang, W. L., Jiang, X. D., Zeng, L., Takeda, Y., . . . Xiao, Z. C. (2008). A TAG1-APP signalling pathway through Fe65 negatively modulates neurogenesis. *Nat Cell Biol, 10*(3), 283-294. doi:10.1038/ncb1690
Meier, S., Bräuer, A. U., Heimrich, B., Nitsch, R., & Savaskan, N. E. (2004). Myelination in the hippocampus during development and following lesion. *Cellular and Molecular Life Sciences CMLS, 61*(9), 1082-1094. doi:10.1007/s00018-004-3469-5
Micheva, K. D., Wolman, D., Mensh, B. D., Pax, E., Buchanan, J., Smith, S. J., & Bock, D. D. (2016). A large fraction of neocortical myelin ensheathes axons of local inhibitory neurons. *Elife, 5*. doi:10.7554/eLife.15784
Miller, R. H., & Fyffe-Maricich, S. L. (2010). Restoring the balance between disease and repair in multiple sclerosis: insights from mouse models. *Dis Model Mech, 3*(9-10), 535-539. doi:10.1242/dmm.001958
Narboux-Nême, N., Goïame, R., Mattéi, M. G., Cohen-Tannoudji, M., & Wassef, M. (2012). Integration of H-2Z1, a somatosensory cortex-expressed transgene, interferes with

the expression of the Satb1 and Tbc1d5 flanking genes and affects the differentiation of a subset of cortical interneurons. *J Neurosci, 32*(21), 7287-7300. doi:10.1523/jneurosci.6068-11.2012

Pelkey, K. A., Chittajallu, R., Craig, M. T., Tricoire, L., Wester, J. C., & McBain, C. J. (2017). Hippocampal GABAergic Inhibitory Interneurons. *Physiol Rev, 97*(4), 1619-1747. doi:10.1152/physrev.00007.2017

Pellerin, L., & Magistretti, P. J. (1994). Glutamate uptake into astrocytes stimulates aerobic glycolysis: a mechanism coupling neuronal activity to glucose utilization. *Proc Natl Acad Sci U S A, 91*(22), 10625-10629. doi:10.1073/pnas.91.22.10625

Peyre, E., Silva, C. G., & Nguyen, L. (2015). Crosstalk between intracellular and extracellular signals regulating interneuron production, migration and integration into the cortex. *Front Cell Neurosci, 9*, 129. doi:10.3389/fncel.2015.00129

Pieke Dahl, S., Kimberling, W. J., Gorin, M. B., Weston, M. D., Furman, J. M., Pikus, A., & Möller, C. (1993). Genetic heterogeneity of Usher syndrome type II. *J Med Genet, 30*(10), 843-848. doi:10.1136/jmg.30.10.843

Plemel, J. R., Michaels, N. J., Weishaupt, N., Caprariello, A. V., Keough, M. B., Rogers, J. A., . . . Yong, V. W. (2018). Mechanisms of lysophosphatidylcholine-induced demyelination: A primary lipid disrupting myelinopathy. *Glia, 66*(2), 327-347. doi:10.1002/glia.23245

Ruden, J. B., Dugan, L. L., & Konradi, C. (2021). Parvalbumin interneuron vulnerability and brain disorders. *Neuropsychopharmacology, 46*(2), 279-287. doi:10.1038/s41386-020-0778-9

Saab, A. S., Tzvetavona, I. D., Trevisiol, A., Baltan, S., Dibaj, P., Kusch, K., . . . Nave, K. A. (2016). Oligodendroglial NMDA Receptors Regulate Glucose Import and Axonal Energy Metabolism. *Neuron, 91*(1), 119-132. doi:10.1016/j.neuron.2016.05.016

Sander, A., Schmelzle, R., & Murray, J. (1994). Evidence for a microdeletion in 1q32-41 involving the gene responsible for Van der Woude syndrome. *Hum Mol Genet, 3*(4), 575-578. doi:10.1093/hmg/3.4.575

Savvaki, M., Panagiotaropoulos, T., Stamatakis, A., Sargiannidou, I., Karatzioula, P., Watanabe, K., . . . Kleopa, K. A. (2008). Impairment of learning and memory in TAG-1 deficient mice associated with shorter CNS internodes and disrupted juxtaparanodes. *Mol Cell Neurosci, 39*(3), 478-490. doi:10.1016/j.mcn.2008.07.025

Savvaki, M., Theodorakis, K., Zoupi, L., Stamatakis, A., Tivodar, S., Kyriacou, K., . . . Karagogeos, D. (2010). The expression of TAG-1 in glial cells is sufficient for the formation of the juxtaparanodal complex and the phenotypic rescue of tag-1 homozygous mutants in the CNS. *J Neurosci, 30*(42), 13943-13954. doi:10.1523/jneurosci.2574-10.2010

Schröck, E., Thiel, G., Lozanova, T., du Manoir, S., Meffert, M. C., Jauch, A., . . . et al. (1994). Comparative genomic hybridization of human malignant gliomas reveals multiple amplification sites and nonrandom chromosomal gains and losses. *Am J Pathol, 144*(6), 1203-1218.

Sekino, Y., Obata, K., Tanifuji, M., Mizuno, M., & Murayama, J. (1997). Delayed signal propagation via CA2 in rat hippocampal slices revealed by optical recording. *J Neurophysiol, 78*(3), 1662-1668. doi:10.1152/jn.1997.78.3.1662

Sloviter, R. S., Sollas, A. L., Barbaro, N. M., & Laxer, K. D. (1991). Calcium-binding protein (calbindin-D28K) and parvalbumin immunocytochemistry in the normal and epileptic human hippocampus. *J Comp Neurol, 308*(3), 381-396. doi:10.1002/cne.903080306

Stedehouder, J., Couey, J. J., Brizee, D., Hosseini, B., Slotman, J. A., Dirven, C. M. F., . . . Kushner, S. A. (2017). Fast-spiking Parvalbumin Interneurons are Frequently Myelinated in the Cerebral Cortex of Mice and Humans. *Cereb Cortex, 27*(10), 5001-5013. doi:10.1093/cercor/bhx203

Takács, V. T., Klausberger, T., Somogyi, P., Freund, T. F., & Gulyás, A. I. (2012). Extrinsic and local glutamatergic inputs of the rat hippocampal CA1 area differentially innervate pyramidal cells and interneurons. *Hippocampus, 22*(6), 1379-1391. doi:10.1002/hipo.20974

Tatu, L., & Vuillier, F. (2014). Structure and vascularization of the human hippocampus. *Front Neurol Neurosci, 34*, 18-25. doi:10.1159/000356440

Thome, C., Roth, F. C., Obermayer, J., Yanez, A., Draguhn, A., & Egorov, A. V. (2018). Synaptic entrainment of ectopic action potential generation in hippocampal pyramidal neurons. *J Physiol, 596*(21), 5237-5249. doi:10.1113/jp276720

Thompson, C. L., Pathak, S. D., Jeromin, A., Ng, L. L., MacPherson, C. R., Mortrud, M. T., . . . Lein, E. S. (2008). Genomic anatomy of the hippocampus. *Neuron, 60*(6), 1010-1021. doi:10.1016/j.neuron.2008.12.008

Wamsley, B., & Fishell, G. (2017). Genetic and activity-dependent mechanisms underlying interneuron diversity. *Nat Rev Neurosci, 18*(5), 299-309. doi:10.1038/nrn.2017.30

Wonders, C. P., & Anderson, S. A. (2006). The origin and specification of cortical interneurons. *Nat Rev Neurosci, 7*(9), 687-696. doi:10.1038/nrn1954

Wyszynski, M., Lin, J., Rao, A., Nigh, E., Beggs, A. H., Craig, A. M., & Sheng, M. (1997). Competitive binding of alpha-actinin and calmodulin to the NMDA receptor. *Nature, 385*(6615), 439-442. doi:10.1038/385439a0

Yermakov, L. M., Hong, L. A., Drouet, D. E., Griggs, R. B., & Susuki, K. (2019). Functional Domains in Myelinated Axons. *Adv Exp Med Biol, 1190*, 65-83. doi:10.1007/978-981-32-9636-7_6

Zinchuk, V., Zinchuk, O., & Okada, T. (2007). Quantitative colocalization analysis of multicolor confocal immunofluorescence microscopy images: pushing pixels to explore biological phenomena. *Acta Histochem Cytochem, 40*(4), 101-111. doi:10.1267/ahc.07002

Zoupi, L., Savvaki, M., Kalemaki, K., Kalafatakis, I., Sidiropoulou, K., & Karagogeos, D. (2018). The function of contactin-2/TAG-1 in oligodendrocytes in health and demyelinating pathology. *Glia, 66*(3), 576-591. doi:10.1002/glia.23266